1 **TITLE**

2 CD2AP is Co-Expressed with Tropomyosin-Related Kinase A and Ras-Related Protein Rab-5A in
3 Cholinergic Neurons of the Murine Basal Forebrain

4

5 **AUTHORS**

6 Lindsey Avery Fitzsimons[1,2] lfitzsimons@une.edu

7 Mohammad Atif-Sheikh[3] matifsheikh@une.edu

8 Jayden Lovely[3] jlovely@une.edu

9 Madison Mueth[2,4] mmueth@une.edu

10 Makaela Rice[2] mrice4@une.edu

11 Kevin Kotredes[5] kevin.kotredes@jax.org

12 Gareth Howell[5] gareth.howell@jax.org

13 Benjamin J Harrison[1,2] bharrison2@une.edu

14

15 1. Biomedical Sciences, College of Osteopathic Medicine, University of New England,
16 Biddeford. ME 04005

17 2. Center for Excellence in the Neurosciences, University of New England. ME 04005

18 3. College of Arts and Sciences, University of New England, Biddeford. ME 04005

19 4. Graduate School of Biomedical Science and Engineering, University of Maine, Orono, ME
20 04469

21 5. The Jackson Laboratory, Bar Harbor, ME 04609

KEYWORDS

CD2AP, cholinergic neurons, Alzheimer's Disease, Rab5, retrograde transport

AKNOWLEDGEMENTS

Funding for these experiments were provided by the National Institutes of Health (R01NS1215; PI: Benjamin J. Harrison) as well as from the University of New England, Center for Pain Research (NIGMS UNE COBRE #P30GM145497; PI: Ian Meng, PhD) and the Khan Foundation through the University of New England, College of Arts and Sciences (Biddeford, Maine, USA). Animal care services were generously provided by UNE COBRE Behavior Core; histology & imaging training and services were provided by the UNE COBRE Histology & Imaging Core Facilities. Both UNE Behavior Core and Imaging & Histology Core facilities are also supported by the UNE Center for Pain Research (NIGMS UNE COBRE #P30GM145497; PI: Ian Meng, PhD). The content is solely the responsibility of the authors and does not necessarily represent the official views of the National Institutes of Health. We wish to thank Christoph Straub for providing numerous tissues and experimental assistance as well as members of the Harrison lab who assisted with imaging, experiments and laboratory management, especially Peter Neufeld, BS. Graphical abstract was created with Biorender.com.

CONFLICT OF INTEREST STATEMENT

The authors declare no competing financial interests.

DATA AVAILABILITY STATEMENT

The data that support the findings of this study are available from the corresponding author upon reasonable request

ABSTRACT

Basal forebrain cholinergic neurons project to the hippocampus and cortex, are critical for learning and memory, and are central to the pathogenesis of Alzheimer's disease (AD). GWAS have consistently shown that genomic variants at the *CD2AP* gene locus are associated with significant increased risk of AD. GWAS studies have also shown that genetic variants in endocytosis genes, including *RAB5A*, significantly increase susceptibility to AD. Previous work in our lab has shown that CD2AP functions as a docking-scaffold/adaptor protein as a coordinator of nerve growth factor (NGF) and trophic signaling in neurons. We have also demonstrated that CD2AP positively regulates Rab5-mediated mechanisms of endocytosis in primary sensory neurons. The purpose of this study was to perform an *in vivo* characterization of CD2AP expression in cholinergic neurons of the brain regions most relevant to AD pathogenesis and to investigate the colocalization of CD2AP and Rab5 in cholinergic neurons of the murine basal forebrain. Brain tissue was perfused, harvested from ChAT^{BAC}-eGFP transgenic mice (N=4 male, N=4 female; aged 10 mo), where cholinergic neurons (co-) express green fluorescence protein (GFP) in central and peripheral neurons that express choline acetyltransferase (ChAT). Frozen tissue sections were used to assess the specificity of the reporter in mouse brain along with localization of both CD2AP and Rab5 (co-) expression using immunofluorescence (IF) analysis of ChAT-GFP+ neurons and primary antibodies against ChAT, CD2AP and Rab5. Image J software was used to develop and optimize a colocalization assay for CD2AP and Rab5 puncta. Experiments were repeated in a follow-up cohort of aged-adult mice (N=2 male, N=2 female; aged 18 mo). IF

expression of CD2AP was quantified in the basal forebrain, diagonal band of Broca (vDB), and striatal regions and compared to results from the cortical regions of the adult mouse brain. Colocalization of CD2AP was observed in the cell bodies of ChAT-GFP+ neurons of the striatum, vDB and basal forebrain regions, where CD2AP expression intensity as well as the number of cell bodies with positive signal increased incrementally. Colocalization analyses revealed near-complete overlap of CD2AP and Rab5 expression in ChAT-GFP+ cholinergic neurons of the basal forebrain region. We conclude that cholinergic neurons express CD2AP in healthy adult and aged-adult mouse brains. These data provide the first evidence of quantifiable CD2AP protein expression of cholinergic neurons specific to the diagonal band of Broca (vDB) and basal forebrain. Together with previous research from our lab, these data support a role for CD2AP in the pathogenesis of AD through orchestration of endocytosis and retrograde signaling. Ongoing studies are underway to verify these findings in a novel AD mouse model that incorporates the humanized variant of *CD2AP*, created by MODEL-AD, where we aim to further investigate how *CD2AP* variants may affect mechanistic components of Rab5 endocytosis as well as subsequent survival of cholinergic neurons in the context of known amyloid beta and Tau pathologies.

1 INTRODUCTION

CD2-associated protein (CD2AP) is a docking-scaffold/adaptor protein with multiple binding interfaces for coordination of protein-protein interactions. It was first characterized as an SH-3-containing protein that binds to CD-2 via the cytoplasmic domain (Dustin et al., 1998; Rouka et al., 2015). CD2AP serves as a hub for signaling pathway components that converge on this scaffold. When the required combination of interactions are formed, the corresponding downstream signaling cascade is activated, and for example, the presence or absence of CD2AP-binding interactions differentially modulates the amplitude of MAPK-ERK or PI3K signal transduction (Kirsch et al., 2001). Known upstream binding-partners include Tropomyosin receptor kinase-A (TrkA) and/or rearranged during transfection (RET); both of are activated by

glial cell line-derived neurotrophic factor (GDNF) family ligands (GFLs) including nerve growth factor (NGF) (Harrison et al., 2016; Tsui & Pierchala, 2008). Known downstream effector binding-partners include the PI3K regulatory subunit p85 (Harrison et al., 2016), p21ras (Qui & Green, 1992) and Akt (Sang et al., 2018).

Endocytosis is a cellular process through which cells absorb proteins on the external surface of the cell by engulfing the molecular contents along with the segment of plasma membrane to form an endosome. Endosomes may subsequently function as mobile compartmentalized signaling platforms termed signalosomes (Hoeller et al., 2005). In neuronal cell populations, retrograde trophic signaling requires endosomal signaling both to internalize the ligand-receptor complex as well as for the propagation/transportation towards its downstream effectors located in the cell body (Delcroix et al., n.d.; Hoeller et al., 2005; Ye et al., 2003).

Variants in genes associated with endocytosis may be neuro-protective, involved in developing resilience against Alzheimer's Disease (AD) (Tesi et al., 2020). Conversely, pathogenic variants have been consistently found in genome-wide association study (GWAS) datasets, as factors associated with increased susceptibility to AD (Lambert et al., 2013; Tesi et al., 2020). Specifically, the *Cd2ap* gene is an AD-predisposition locus, substantiated by multiple GWAS with multiple populations (African American (Kunkle et al., 2021; Sherva et al., 2023), Chinese (Xue et al., 2022), Northern and Western European ancestry (CEU)(Gockley et al., 2021), UK Biobank (Khaire et al., 2022; Marioni et al., 2018)) that support the association of *Cd2ap* variants with small but significant increases in incidence (Amlie-Wolf et al., 2019), progression (Amlie-Wolf et al., 2019; van Bree et al., 2022), and severity (van Bree et al., 2022; Xue et al., 2022) of Alzheimer's Disease (AD). CD2AP is expressed by multiple cell types in multiple tissue types (Li et al., 2000), and may play a role in several mechanisms responsible for the pathogenesis and/or progression of AD. For example, dysfunction of brain vasculature is a pathophysiological mechanism of blood brain barrier deficits (Cochran et al., 2015) relevant to multiple dementias, including AD, and is a well-established source of CD2AP expression (Asghari

120 et al., 2024; Koizumi et al., 2016; Liu et al., 2024). Outside of the vasculature, CD2AP is known to
121 be expressed by migratory dendritic cell populations (Li et al., 2000; Schaefer et al., 2017), renal
122 podocytes (Li et al., 2000; Schwarz et al., 2001), and sensory neurons of the peripheral nervous
123 system (Harrison et al., 2016). Thus, the translational relevance of GWAS studies of *Cd2ap* must
124 be interpreted carefully, and should serve as a confirmation of the relevance of endocytosis and
125 retrograde transport in AD. However, the mechanistic underpinning of *Cd2ap* variant-associated
126 risk, specific to the dynamic interplay between/among cell and tissue types remain poorly
127 characterized.

128 It is widely accepted that phosphorylated Tau protein, forming neurofibrillary tangles, impedes
129 conductance and function of neurons, resulting in the neurotoxicity and degradation seen in
130 healthy aging as well as in neurodegenerative disease like AD (Dickson et al., 1986; Kovacs et
131 al., 2017). A genetic association between CD2AP, tau-accumulation and subsequent neurotoxicity
132 (Nisbet et al., 2015) have been observed using drosophila homolog *cindr* in *a* loss of function
133 model of AD (Nisbet et al., 2015; Shulman et al., 2014). CD2AP scaffolding interactions regulate
134 Rab5-mediated endocytosis (Behl et al., 2022; Cormont et al., 2003a; Furusawa et al., 2019;
135 Gockley et al., 2021; Maninger et al., 2024; Rouka et al., 2015; Shen et al., 2020; Xu et al.,
136 2018a). Therefore, reduced CD2AP function may lead to impaired clearance and subsequent
137 accumulation of amyloid-beta (Aß) and tau aggregates (Behl et al., 2022).

138 Reduced kidney function and diagnosis with chronic kidney diseases (CKD) is an
139 established risk factor for cognitive decline and AD, although the mechanism has yet to be fully
140 elucidated (Nakagawa et al., 2017; Shi et al., 2018; Zhang et al., 2020). The biochemistry and
141 function of CD2AP was first characterized in T-lymphocytes of the immune system, where it was
142 described as an adhesion molecule responsible for mechanisms of protein segregation and
143 cytoskeletal polarity, and where it was first postulated to orchestrate dynamics of receptor
144 patterning via the cytoskeletal scaffold (Dustin et al., 1998). This initial characterization prompted
145 further exploration of CD2AP expression. In other cell and organ systems, and specifically in the

podocyte cells of the kidney, a highly-specialized, gate-keeping cell found in the glomerulus (Dustin et al., 1998; Nakagawa et al., 2017; Shi et al., 2018; Shih et al., 1999; Zhang et al., 2020). In podocytes, CD2AP is located to the actin-rich scaffolds of the slit-diaphragm, a charge-selective opening through which vascular/metabolic waste products are filtered from circulating blood and excreted from the body in urine. Loss of CD2AP is homozygous-lethal, due to the rapid-onset of severe nephrotic syndrome and glomerular disease, resulting in kidney failure and death in mice by 6 weeks of age due to failure of the slit-diaphragm (Li et al., 2000; Shih et al., 1999). Thus, CD2AP functions as a mediator and organizer of F-Actin structures, where it colocalizes with Rab4 in podocyte endosomes (Welsch et al., 2001, 2005). Genetic mutations and/or impairment of CD2AP, therefore, not only impairs cellular cytoarchitectural scaffolding, but also decreases endosomal-mediated degradation processing, influencing secretase and amyloid precursor proteins (APP) transport and ultimately enabling the accumulation of APP segments and tangles (Behl et al., 2022; Howe & Mobley, 2004; Iulita & Cuello, 2016).

CD2AP is also required for the maintenance of structure and permeability of systemic blood vessels (e.g. epithelial and endothelial cells) (Hamano et al., 2002; Li et al., 2000; Vandal et al., 2022). Interestingly, analysis of microvessels isolated from human patients with confirmed AD observed *Cd2ap* expression to be linearly associated with cognitive decline and *Cd2ap* KO from brain microvasculature (microvessels) in mice resulted in cognitive impairment (Vandal et al., 2022). Interaction between the vasculature and the immune system has also been implicated in the onset, progression and severity of AD (Bettcher et al., 2021; Heppner et al., 2015). In vascular endothelial cells CD2AP regulates intercellular adhesion molecule-1 (ICAM-1) (Schaefer et al., 2017). Loss of CD2AP initiates increased clustering of ICAM-1 on the endothelial cell surface, leading to excessive leukocyte transmigration and subsequent pro-inflammatory signaling pathways associated with kidney dysfunction, arthritis and atherosclerosis (Schaefer et al., 2017). CD2AP has also been shown to be highly expressed in plasmacytoid dendritic cells (pDC), a

171 specialized subtype of dendritic cells known to initiate type-1 interferon signaling in response to
172 inflammation and in microbial pattern recognition (Srivatsan et al., 2013).

173 In neuronal cell populations, CD2AP has been shown to be expressed in embryonic dorsal
174 root ganglia (DRG) in E11 mouse embryos, and was identified as a key regulator molecule for
175 growth factor and hormone-mediated cell signaling mechanisms critical for mammalian
176 organogenesis and embryogenesis as a whole (Lehtonen et al., 2008). Previous studies from our
177 laboratory have demonstrated that CD2AP is expressed in mature primary sensory neurons of the
178 adult peripheral nervous system *in vivo (Harrison et al., 2016)*. Stimulation of these cells with
179 nerve growth factor (NGF), initiated CD2AP binding to Neurotrophic Receptor Tyrosine Kinase 1
180 (Gene name *Ntrk1*, Protein name: Tropomyosin Receptor Kinase A (TrkA)) and the PI3-kinase
181 effector (p85) , to upregulate the PI3K/AKT pathway, further demonstrating a functional role for
182 CD2AP as a positive coordinator of NGF-stimulated axon growth and branching (Harrison et al.,
183 2016). More recent experiments investigating the Ras and Rab Interactor 3 (RIN3), have
184 demonstrated that CD2AP is expressed in murine cholinergic neurons isolated from basal
185 forebrain, and that endosomal trafficking involving CD2AP *in vitro*, is reliant upon RIN3, a guanine
186 nucleotide exchange factor (GEF) in the Rab5 small GTPase family (Yoshida et al., 2021).
187 CD2AP has also been characterized in the nervous system of *Drosophila,* via its homologue, *cindr*
188 (Ojelade et al., 2019). *Cindr* expression can be found in adult *Drosophila* throughout the
189 brain/nervous system, and is predominantly expressed within neuropil and the surrounding
190 presynaptic terminals, where it is shown to function as a positive regulator and rate-limiting
191 component of synaptic transmission, calcium release, and proteostasis (Ojelade et al., 2019).
192 Silencing of *cindr* (CD2AP) robustly enhanced tau-toxicity in *Drosophila* (Shulman et al., 2014),
193 using a human mutant form of Tau shown to be associated with familial frontotemporal dementia
194 (Wittmann et al., 2001).

195 Previously, we observed that CD2AP is expressed in primary sensory neurons, and
196 demonstrated that this adaptor protein coordinates NGF-TrkA-PI3K trophic signaling and

197 retrograde transport via Rab5-decorated endosomes (Harrison et al., 2016). In the current study,
198 we observed that in central nervous system (CNS) neurons, CD2AP expression is predominantly
199 expressed in populations of cholinergic neurons in the basal forebrain and striatum. Cholinergic
200 projections from the basal forebrain to the cortex constitute the primary source of cholinergic input
201 to the forebrain (Engelhardt et al., 2007), and are also known to be the first to show signs of
202 degeneration in AD (Geula et al., 2021). Disruption of NGF-TrkA trophic signaling via interruption
203 of retrograde Rab5a endosomes is a key mechanism of AD pathogenesis (Iwano et al., 2023). We
204 therefore also examine the localization of CD2AP and TrkA with Rab5a endosomes in cholinergic
205 neurons and discuss a possible role for CD2AP in the trophic support of cholinergic neurons and
206 AD pathophysiology.

207

208 **2 MATERIALS AND METHODS**

209 **2.1 Animals**

210 Animal housing and procedures were approved by the Institutional Animal Care and Use
211 Committee of the University of New England consistent with federal regulations and guidelines. All
212 animals used for this study were ChAT^{BAC}-eGFP mice (JAX Strain# 007902) purchased from The
213 Jackson Laboratory (Bar Harbor, Maine). Age and sex of cohorts are specified in appropriate
214 sections below.

215 **2.2 Prediction of CD2AP mRNA Expression in Neuronal Populations**

216 The DropViz online search tool was used to uncover putative populations of *Cd2ap*-expressing
217 adult mouse neurons (Saunders et al., 2018). The “Limit by Class” option was set to “Neuron” and
218 the top-10 results were retrieved using following individual search terms: “*Cd2ap*”, “*Ntrk1*” and
219 “*Chat*”. Results reflect the top-10 expressing populations for each of these individual search
220 terms.

221 **2.3 Tissue Preparation & Frozen Tissue Sectioning**

222 Six week-old, ChAT-GFP:Cre-+ mice (N=2 males, 2 females), were deeply anaesthetized with
223 0.1ml intraperitoneal Euthasol, before intracardial perfusion with 20ml phosphate buffered saline
224 (PBS) followed by 30ml cold 4% paraformaldehyde in PBS. Brains were immediately harvested,
225 and post fixed in cold 4% paraformaldehyde in PBS for 4 hours. Following fixation, tissues were
226 washed with PBS and incubated in 30% sucrose cryoprotectant for 48 hours. Tissues were then
227 embedded in OCT frozen tissue embedding medium and stored at -80 degrees Celsius prior to
228 sectioning. Coronal sectioning of mouse brains embedded in OCT was performed using a Leica
229 Cryostat 1900 (Leica Microsystems, USA). From each mouse, fifteen 12um thick, coronal brain
230 sections were sliced 1.77mm to 0.13mm rostral to the bregma onto a glass slide (VWR®,
231 Superfrost® Plus Micro Slide, Cat# 48311-703).

232 **2.4 Tissue Processing and Immunofluorescent Staining**

233 Sections were dried overnight, then briefly washed with PBS before incubation with blocking
234 solution (4% normal donkey serum, 0.3% Triton X-100 PBS) for 30 mins at room temperature.
235 Following blocking, slides were incubated with primary antibodies at the indicated dilutions over-
236 night (18 hours) at room temperature (Table 1). Slides were then washed 5 times for 5 minutes
237 with washing buffer (0.3% Triton X-100 in PBS) before incubation with fluorescent secondary
238 antibodies (Table 1) at room temperature for 1 hour. Finally, slides were washed 5 times for 5
239 minutes with washing buffer (0.3% Triton X-100 in PBS) before mounting with Fluoroshield
240 Mounting Medium with DAPI (Abcam, Cat# ab104139) using 1.5 thickness coverslips. The
241 following primary antibodies were used: Anti-Cd2ap (Proteintech, Cat# 51046-1-AP,
242 RRID:AB_2879436); anti-TrkA (R&D, Cat# AF1056, RRID:AB_2283049); anti-choline
243 acetyltransferase (ChAT; Sigma-Aldrich, Cat# AB144P, RRID:AB_2079751); anti-green
244 fluorescence protein (GFP; Aves Labs, Cat# GFP-1020, RRID:AB_10000240); and anti-Rab5
245 (Cell Signaling Technology, Cat# 46449, RRID:AB_2799303).

246 **2.5 Thick tissue Immunofluorescence (iDISCO)**

247 Preliminary characterization was performed using thick tissue sections (150µm) of ChAT-
248 GFP:Cre+ mouse brains embedded in 5% agarose in 1X PBS. Thick sections were cleared and
249 prepped for IF using iDISCO (Renier et al., 2014). Whole-section images of Chat-GFP+ brains
250 were imaged at 20X magnification using an epifluorescence microscopy slide scanner and images
251 were merged to generate a composite using the image stitching function (BZ-X800 Slide
252 Scanning Microscope, Keyence, USA). Working concentrations of primary and secondary
253 antibodies were increased for thick tissue section IF and are indicated in Table 1**.**

254

255 **TABLE 1** Antibodies and reagents used for immunofluorescence analysis.

256

257 **2.6 CD2AP Antibody Validation**

258 The anti-CD2AP primary antibody (Proteintech, Cat# 51046-1-AP, RRID:AB_2879436) was
259 validated for use with qualitative and quantitative IF in two previous studies. Characterization of
260 this antibody was performed using fixed, frozen sections of mouse kidney tissue, demonstrating
261 signal specificity localized along the glomerular basement membrane, as expected (Yoshida et
262 al., 2021). Subsequent validation of anti-Cd2ap was performed using Lentiviral-mediated, *Cd2ap*-
263 knockdown tissue in human telomerase-immortalized retinal pigmented epithelial cells (hTERT-
264 RPE1) as well as murine NIH3T3 cells (Iwano et al., 2023). Investigators demonstrated that
265 expression of CD2AP was localized to the primary cilium in control cells, and was ablated in
266 knockdown tissues using both IF (See Figure 5, panels A-C, Iwano et al., 2023) and Western Blot
267 (See Figure 5, panel E Iwano et al., 2023). Additional antibody validation was performed in our
268 laboratory, using kidney tissue collected from ChAT-GFP+ mice, fixed and processed for frozen
269 tissue sectioning.

270 **2.7 Quantification of CD2AP Fluorescence**

271 2.7.1 Microscopy and Image Analysis

272 One slide/mouse (with all 15 sections) was imaged using an epifluorescence microscope (Leica
273 DMi8, Leica Microsystems) at 20X. Four color micrographs from alternate (odd numbered)
274 sections were then processed using FIJI software (ImageJ2; version 2.14.0/1.5f) (Rueden et al.,
275 2017). For fluorescence measurements in ChAT-GFP positive neurons, a binary mask was
276 created by thresholding the GFP channel. The mask was processed to remove noise by removing
277 foci<20μm in diameter. Masks were then layered over the ChAT antibody stain and then the
278 CD2AP antibody stain to acquire the respective fluorescent signals from GFP-positive neurons.

279 2.7.2 Estimation of Background Fluorescence

280 Populations of cell bodies of developing cholinergic neurons undergo a phenotypic switch into
281 adulthood, where multiple cholinergic cell subtypes are thought to be established based on
282 synaptic properties (Ahmed et al., 2019). In ChAT/GFP+ mice, GFP signals are sustained into
283 adulthood (Tallini et al., 2006), and represent a subpopulation of cortical interneurons which
284 synapse locally within the cortex, and are best characterized by their expression of vasoactive
285 intestinal peptide (Ahmed et al., 2019; Engelhardt et al., 2007). In the present study, we confirm
286 that this population of adult cortical neurons remain ChAT-GFP positive, but do not stain with
287 ChAT antibody. Therefore, we measured the background fluorescence of antibody stains using
288 signals from GFP-positive ChAT-negative neurons.

289 **2.8 Immunofluorescence Colocalization Assays**

290 Colocalization assays were performed on IF z-stack images collected using confocal microscopy
291 (Leica Stellaris) and Image J *EzColocalization* plugin (Stauffer et al., 2018). To restrict analysis to
292 Chat-GFP+ neurons, the polygon selection tool was used to trace the outline of the ChAT-GFP+

293 cell body from the GFP+ maximum projection, and the 'region of interest' (ROI) manager was
294 employed to demarcate the GFP+ border onto the Cd2ap (yellow) and Rab5 (magenta) split
295 channel maximal projections. Selection of images was restricted to those collected in the vDB
296 region of the basal forebrain, and an average of 10 images per section, 20 sections per animal, in
297 a total of 4 ChAT-GFP+ mice.

298 **2.9 Statistical Analysis**

299 All statistical analyses were conducted using Graphpad Prism 9. Data are presented as
300 individual animal regional mean values ± standard deviation (SD) and reflect quantification of
301 integrated density of fluorescence intensity, measured using FIJI (ImajeJ2). Collated data from
302 grouped animals was expressed as mean regional values ± standard error of the mean (SEM).
303 Data normality for individual animals as well as grouped data ware analyzed and confirmed using
304 the Kolmogorov-Smirnov test. Regional quantification of CD2AP expression was compared
305 between brain regions using a standard one-way analysis of variance (ANOVA) followed by
306 Tukey's post-hoc analysis. For all analyses, statistical significance was set at $p<0.05$.

307 For immunofluorescence colocalization assays, degree of overlap for CD2AP and Rab5
308 punctuate colocalization was assessed using the R value calculated from Pearson correlation,
309 analysis. Additional analysis of colocalization degree of overlap was assessed using a Costas
310 array, and statistical significance of the Costas P value was $p<0.05$.

311

312 **3 RESULTS**

313 **3.1 Analysis of Publicly Available Single-Cell Sequencing Data Reveals that *Cd2ap* mRNA**
314 **is Expressed in TrkA-Expressing Cholinergic Neurons**

315 Our previous work provided one of the first descriptions of the structural and mechanistic
316 dynamics of CD2AP in neurotrophin-mediated neuroplasticity, coordination of scaffolding

317 interactions between TrkA and AKT subunit p85 in neurons and the positive regulation of
318 retrograde signaling implemented through Rab5-decorated signalosomes (Harrison et al., 2016).
319 We further postulated that the retrograde, Rab5-mediated signaling mechanism, combined with
320 the dynamics of the CD2AP-TrkA complex in cholinergic neurons would be a reasonable,
321 potential mechanism(s), highly applicable to the pathogenesis of neurodegenerative disease like
322 AD (Harrison et al., 2016). Since this publication, germline variants in human *CD2AP* have
323 remained at the forefront of GWAS investigating risk(s) for development of AD in humans (Latina
324 et al., 2023; Rajabli et al., 2023; Xue et al., 2022).

325 The functional consequences of *Cd2ap* variants as well as the possibility of a potential role
326 of CD2AP in CNS neurons is currently unknown. Using human AD GWAS studies, we first
327 performed a review of the literature generated, with an emphasis on recent GWAS studies
328 published between 2021 to present (date of submission, June 2024). Since 2021, we report a total
329 of five GWAS studies for AD that identify *CD2AP* as a primary risk factor (and risk factor loci) for
330 the development of AD in humans (Table 2). Of the loci identified, specific variant rs9349407 was
331 correlated with increased risk for AD in Chinese populations (Gao et al., 2022) and specific variant
332 rs7738720 was correlated with increased risk of AD pathophysiology in individuals of African
333 ancestry (Sherva et al., 2023). Overall, we identified a total of 19 GWAS studies performed
334 worldwide (since the year 2010) where *CD2AP* loci have been positively associated with AD
335 pathophysiology (Table 2).

336

337 **TABLE 2** Summary of GWAS studies from 2013 to present (June 2024) implicating *CD2AP* in the
338 pathogenesis and/or susceptibility to AD in humans.

339

340 Although there is a clear association between *Cd2ap* variants and an increased risk of AD,
341 it is currently unknown if *Cd2ap* (mRNA) or CD2AP (protein) is expressed in neurons of the CNS

342 in either mouse or human models of health and disease. In order to determine and characterize
343 CD2AP expression in CNS neurons, we performed an analysis of single-cell, neuronal, RNA-
344 sequencing data publicly-available and sourced from DropViz webtool (Saunders et al., 2018)
345 (Table 1). Our initial analysis of neuronal cell types ordered neurons by level of CD2AP
346 expression (Figure 1, magenta), expressed as transcripts per 100,000 in cluster. From these data,
347 we found that of the few neuronal populations expressing CD2AP, these neurons also expressed
348 the highest levels of *Ntrk1 (TrkA),* classifying them as cholinergic neuronal cell populations
349 (Figure 1**,** cyan). Highest expression levels of *Ntrk1* were found in cholinergic interneurons of the
350 striatum (Figure 1), along with neurons located in the globus pallidus (GP; Figure 1). Striatum
351 interneurons and GP neurons were found to also co-express the highest values of *Cd2ap* in the
352 top-10, highest Ntrk1-expressing (cholinergic) neurons of the adult mouse brain (Figure 1). In
353 other words, of all neuronal cell types present in the adult mouse brain, *Cd2ap* expression was
354 restricted to Trk-A expressing, cholinergic neurons (Figure 1).

355 **3.2 CD2AP Protein is Expressed in Cholinergic Neurons of the Murine Basal Forebrain**

356 To determine if CD2AP is expressed in ChAT neurons, (as predicted in Figure 1), we
357 performed an immunofluorescence analysis of frozen tissue sections from ChAT-GFP reporter
358 (ChAT-GFP+) mouse brains (Figure 2). Whole-section analysis of ChAT-GFP+ brains confirmed
359 the bilateral presence and expression of ChAT-GFP+ neurons throughout the superior thalamic
360 radiation (striatum), nucleus accumbens and substantia innominata (Figure 2, a). CD2AP
361 expression was highest in the basal forebrain region, where we observed the presence of ChAT-
362 GFP+ neurons (cyan) throughout the vDB. Co-localization of ChAT-GFP+ and anti-ChAT (yellow)
363 in presumed-cholinergic neurons of the vDB confirmed the specificity of the ChAT primary
364 antibody, as well as provided confirmation that these neurons are, in fact, acetylcholine-producing
365 (Figure 2). Of note, absence of ChAT+ staining (yellow) in Chat-GFP+ cell bodies (cyan) of the
366 cortical region also confirmed the specificity of the anti-ChAT antibody, as was originally
367 documented by Gamage and colleagues in their recent characterization of the ChAT-GFP

368 transgenic mouse brain (Gamage et al., 2023). The presence of ChAT-GFP+/anti-ChAT-negative
369 cell bodies in the cortex therefore serves as an effective, internal negative control tissue, and as
370 an additional verification for the specificity of the anti-ChAT antibody.

371 Next, we sought to quantify expression of CD2AP in cholinergic populations (Figure 3).
372 Confocal scans were collected from the following regions of adult mouse brains (N=4): Substantia
373 innominata (basal forebrain) region, vDB, the superior thalamic radiation (striatum), and the cortex
374 (Figure 3). Three-channel fluorescence signals were acquired from ChAT-GFP reporter (cyan),
375 CD2AP antibody (magenta) and ChAT antibody (yellow; Figure 3). Double-positive signal from
376 CD2AP and ChAT antibodies, were detected in the majority of ChAT-GFP+ cell bodies in the
377 basal forebrain, vDB and striatum (Figure 3). ChAT-GFP+ soma in the cortex region did not stain
378 with the anti-ChAT antibody (yellow). ChAT is expressed during a developmental window in
379 cortical neurons, and therefore, in the adult these neurons are ChAT-GFP+ and ChAT-antibody
380 negative (Gamage et al., 2023). Therefore, this served as a convenient negative control to
381 quantify background signals from ChAT and CD2AP antibody immunostaining. Note that,
382 although, CD2AP signal was not present in the cell bodies of cortical CHAT-GFP neurons, it was
383 expressed in cortical vascular structures and non-neuronal cells, as expected (Vandal et al.,
384 2022). Taken together, these results validate the specificity of CD2AP immunostaining, and
385 qualitatively show that CD2AP is co-expressed with ChAT in the substantia innominata (basal
386 forebrain), vDB, and striatum.

387 To quantify CD2AP expression, we used the imaging data documenting regional
388 distribution of CD2AP+ fluorescence in ChAT-GFP/ChAT-double-positive cells (Figure 3) and
389 performed a one-way ANOVA to compare and contrast CD2AP integrated density values in the
390 cortex (negative control), superior thalamic radiation, substantia innominata (basal forebrain) and
391 Broca's area (vDB; Figure 4, a-b). CD2AP fluorescence (integrated density) values of individual
392 animals were expressed as mean values ± SD (Figure 4, a), and collated group regional data
393 were expressed as mean values ± SEM (Figure 4, b). In the grouped regional mean data, the

394 lowest CD2AP fluorescence (mean integrated density ± SEM) was observed in the cortex (3449 ±
395 124), serving as a baseline/background measurement. Mean signal intensity from the superior
396 thalamic radiation was 4936± 27.6, the substantia innominata (basal forebrain) was 7428 ± 55.9
397 and Broca's area/vDB was 10929 ± 72.3 (Figure 4, b). A one-way ANOVA with Tukey post-hoc
398 analysis revealed a statistically significant difference among brain regions (p=0.0004).
399 Fluorescence expression of CD2AP was significantly higher in the Broca/vDB regions when
400 compared to background cortex (p=0.0085; Figure 4, b). Mean CD2AP expression in the vDB was
401 also statistically significantly greater when compared to the superior thalamic radiation
402 (p=0.0018), and the basal forebrain (p=0.04; Figure 4, b).

403 **3.3 CD2AP is Colocalized to the Termini of Cortical Projections of ChAT-GFP+ Basal**
404 **Forebrain Neurons**

405 During the quantification of CD2AP fluorescence expression, we observed an overlap in
406 signaling between CD2AP (magenta) and ChAT-GFP+ projections extending from the basal
407 forebrain up through the isocortical regions. Subsequent focused analyses sought to substantiate
408 these observations with the use of immunofluorescence to more thoroughly document CD2AP co-
409 expression with ChAT-GFP+ signal beginning with ChAT-GFP+ cell bodies in the basal forebrain
410 and continuing throughout the neuronal projections extending anteriorly and superiorly in
411 proximity to the hippocampus and within the isocortex (Figure 5). Preliminary analysis of thick
412 tissue sections from ChAT-GFP:Cre+ brains allowed investigators to characterize and visualize
413 both the spatial and dimensional layout of ChAT-GFP+ neurons, along with their respective
414 neuronal projections and termini from a three-dimensional perspective (Figure 5, top).

415 Confocal microscopy analysis of ChAT-GFP+ cell bodies was repeated to confirm the co-
416 labeling of ChAT-GFP+ (cyan) and CD2AP+ (magenta; magenta and cyan overlap is white) signal
417 in the cell bodies of cholinergic neurons of the basal forebrain (Figure 5, bottom left). Subsequent
418 analyses of ChAT-GFP+ neuronal projections from the basal forebrain confirmed the presence of

419 co-labeling with CD2AP in these cholinergic fibers (Figure 5**,** bottom right). Of note, vascular
420 expression of CD2AP is substantial and can easily be visualized throughout all regions of the
421 mouse brain. However, CD2AP co-labeling in ChAT-GFP+ projections are visualized in a
422 morphological pattern and smaller/finer distribution of specific staining that is morphologically
423 distinctive from CD2AP+ expression in blood vessels (Figure 5, bottom).

424 **3.4 CD2AP is colocalized with Rab5-Positive, Early Endosomal Formations of ChAT-GFP+**
425 **Basal Forebrain Neurons.**

426 To further examine CD2AP expression in cholinergic neurons, relative to endosomal
427 formation, we performed a series of immunofluorescence experiments to characterize and
428 quantify CD2AP colocalization with Rab5, a small GTPase, mediator and sorter of endosomal
429 formation (Figure 6). Immunofluorescence analysis of ChAT-GFP+ brain frozen tissue sections
430 revealed an abundance of CD2AP (yellow) and Rab5 (magenta) colocalization puncta, which
431 were interpreted as formed endosomes, and which were diffusely present in ChAT-GFP+ neurons
432 (cyan) throughout the basal forebrain tissue. CD2AP-Rab5-positive (CD2AP/Rab5+) endosomes
433 observed throughout the cell body of the ChAT-GFP+ neurons and are indicated by a white
434 arrowhead (Figure 6, a). We also observed clusters of CCD2AP/Rab5+ endosomes that did not
435 overlap with the ChAT-GFP+ signal of the ChAT-GFP+ cell bodies and were indicated by a red
436 arrowhead (Figure 6, b). In order to quantify colocalization of CD2AP (yellow) with Rab5+ vesicles
437 (magenta), we performed colocalization analyses of ChAT-GFP+ cell bodies (cyan; Figure 6).
438 Quantification of CD2AP/Rab5+ colocalization revealed a near-complete overlap between
439 CD2AP+ and Rab5+ punctuates (Figure 6). Mean Pearson correlation R values was 0.80, with a
440 Costas P value of 1.00, demonstrated in Figure 6.

441

442 **4 DISCUSSION**

443 By analysis of publicly available scRNA-seq data, we observed inherent expression of
444 *Cd2ap* specifically and exclusively in Trk-A expressing, cholinergic neurons of the central nervous

system. Using an *in vivo* reporter mouse for ChAT-GFP-positive cholinergic neurons, we confirmed the presence and distribution of ChAT/GFP+ neurons in the superior thalamic radiation (striatum), nucleus accumbens/substantia innominata, the basal forebrain, and the vDB. Additionally, we identified and quantified the colocalization/expression of ChAT/GFP+/ChAT+ with CD2AP in cholinergic neurons in each of these regions, most pronounced of which was quantified in the vDB/basal forebrain. Notably, expression of CD2AP in ChAT/GFP+ axonal branching/termini continues outside of the basal forebrain and up through the (iso-) cortex, posing additional hypotheses surrounding a possible role/application for CD2AP in retrograde axonal transport signaling in maintaining the viability and bidirectionality of basal forebrain communication with the cortex in healthy aging and in AD pathogenesis. Co-staining of ChAT-GFP+/CD2AP+ cell bodies with an antibody against Rab5 revealed near-complete colocalization between CD2AP and Rab5 punctuate patterning, consistent with endosomal structural configurations previously described in primary sensory neurons of the peripheral nervous system and in cholinergic neurons *in vitro* (Harrison et al., 2016; Shen et al., 2020). In this study, we are the first to characterize the expression of the Alzheimer associated gene, *Cd2ap,* in populations of adult CNS neurons, *in vivo*.

CD2AP was first characterized as an adhesion molecule critical for the structural integrity, filtration and overall function of the kidney, as determined using various genetic knockout/knock-down studies *in vivo* and *in vitro* (Li et al., 2000; Schwarz et al., 2001; Shih et al., 1999). Concurrently, CD2AP was identified as a genetic risk factor for the development of AD in humans (Hollingworth et al., 2011; Naj et al., 2011), a finding that has been supported by a substantial number of studies across model organism species, including *Mus musculus* (Vandal et al., 2022), *Drosophila* (Ojelade et al., 2019; Shulman et al., 2014), and *Caenorhabditis elegans* (Alvarez et al., 2022; Kim et al., 2018). Previously established *Cd2ap* variants have even been incorporated along with variants in *Trem2*^{em1Adiuj}, *App*^{em1Adiuj} and *Apoe*$^{tm1.1(APOE*4)Adiuj}$ into a multi-genetic/causal, humanized mouse model of AD (JAX Strain# 033873) (Jung et al., 2023; Pandey et al., 2023).

471 Although CD2AP is known to be expressed in tissues and cell types outside of the kidney (e.g.
472 primary sensory neurons (Harrison et al., 2016), endo/epithelial cells (Cochran et al., 2015; Li et
473 al., 2000) and migratory glial cells (Bao et al., 2012; Vandal et al., 2022), inherent expression of
474 CD2AP in cholinergic neurons of CNS (*in vivo*) has not previously been identified or quantified,
475 supporting the plausibility of a pathogenic mechanism of AD inherent to cholinergic neurons of the
476 CNS.

477 Early characterizations of CD2AP (previously also referred to as 'Cas ligand with multiple
478 Src homology (SH) 3 domains' (CMS)) identified that co-expression of active Rab4 and CD2AP *in*
479 *vivo* resulted in the enlargement of early endosome formations, was required (along with c-Cbl)
480 for proper endosomal formation, and finally, that CD2AP interactions with both Rab4 and Rab7
481 might also be involved in degradation of these endosomes (Cormont et al., 2003b). Interestingly,
482 CD2AP expression in conditionally immortalized mouse podocytes was shown to be directly co-
483 expressed with Rab4, but not Rab5, in late-endosomal processing (Welsch et al., 2005).
484 However, subsequent research from our laboratory and others, has indicated that CD2AP
485 interaction with specific Rab isoforms may, in fact, vary by cell/tissue type, where NGF signaling
486 via TrkA receptor in primary, DRG neurons, is dependent upon TrkA+/Rab5+ endosomes for
487 mediation of long-range NGF signaling (Furusawa et al., 2019; Harrison et al., 2016). In the
488 present study, we document the visual and quantitated colocalization of CD2AP and Rab5 *in vivo,*
489 where previous research has identified interactions with Rab3 (Iwano et al., 2023), Rab4
490 (Furusawa et al., 2019), and RIN (Rouka et al., 2015; Shen et al., 2020) or isolated with Rab5 *in*
491 *vitro* (Furusawa et al., 2019; Rouka et al., 2015). Evidence in support of a role for Rab5
492 specifically for endosomal formation and the propagation of trophic signaling in cholinergic
493 neurons (Behl et al., 2022; Harrison et al., 2016; Kawabata, 2022), in conjunction an established
494 association of impaired Rab5 signaling in brain tissue of deceased humans with confirmed AD (Xu
495 et al., 2018b), are consistent with the findings of the present study, and further support the

496 hypothesis that CD2AP-Rab5 endosomal signaling in cholinergic neurons of the basal forebrain is
497 a viable, mechanistic explanation for AD pathogenesis.

498 In the nervous system, CD2AP plays a regulatory role in neuronal cell survival
499 mechanisms, a process that is known to be trophic-factor dependent (Tsui & Pierchala, 2008).
500 Early investigations into the possible pathological relevance of trophic signaling in AD showed that
501 while retrograde transport was reduced, there is a specific reduction in NGF retrograde transport
502 observed from the hippocampus to the septum in basal forebrain cholinergic neurons in a Ts65Dn
503 mouse model of Down's Syndrome, also known to be applicable to mouse models of AD (Cooper
504 et al., 2001). In addition to what is known about CD2AP, Rab5-mediated endocytosis is also
505 hypothesized to be dysregulated in AD (Pensalfini et al., 2020; Xu et al., 2018b), a finding that is
506 also supported by human GWAS studies (Novikova et al., 2021; Tesi et al., 2020).

507 In the present manuscript, we reiterate the origin and pathogenic significance of
508 cholinergic neurons in AD, where current working hypotheses support the idea that disruption of
509 endocytosis may lead to accumulation of amyloid beta and/or the formation of neurofibrillary
510 tangles. We highlight and summarize the volume of GWAS studies supporting the idea that
511 variants in genes known to be critical for endocytosis and endocytic processes (like *Cd2ap* and
512 *Rab5*) and that are consistently associated with increased susceptibility to AD. We summarize
513 previous studies from our laboratory and others, supporting a role for CD2AP as a coordinator of
514 NGF signaling. Finally, we present new data demonstrating that CD2AP is expressed in both the
515 cell body as well as localization in the projections of cholinergic neurons in the CNS, reiterating
516 the working hypothesis that CD2AP may orchestrate endocytosis in cholinergic neurons and
517 formalizing the feasibility and relevance of this mechanism to AD pathogenesis.

518

519 **5 CONCLUSION**

520 CD2AP is expressed in multiple cell types critical for the function of various tissues/organs
521 like those of the kidney, vasculature, immune system, sensory neurons of the PNS, and now,
522 cholinergic neurons of the CNS. Taken together, we propose a working model through which the
523 targeting CD2AP-coordinated signals may serve as a viable target to prevent endocytosis-
524 mediated mechanisms of neurodegeneration and may also serve as a multifactorial, systems-
525 wide approach to improving AD outcomes.

526

527 **REFERENCES**

528 Ahmed, N. Y., Knowles, R., & Dehorter, N. (2019). New Insights Into Cholinergic Neuron Diversity. *Frontiers*
529 *in Molecular Neuroscience*, *12*, 204. https://doi.org/10.3389/fnmol.2019.00204
530 Alvarez, J., Alvarez-Illera, P., Santo-Domingo, J., Fonteriz, R. I., & Montero, M. (2022). Modeling
531 Alzheimer's Disease in Caenorhabditis elegans. *Biomedicines*, *10*(2), Article 2.
532 https://doi.org/10.3390/biomedicines10020288
533 Amlie-Wolf, A., Tang, M., Way, J., Dombroski, B., Jiang, M., Vrettos, N., Chou, Y.-F., Zhao, Y., Kuzma, A.,
534 Mlynarski, E. E., Leung, Y. Y., Brown, C. D., Wang, L.-S., & Schellenberg, G. D. (2019). Inferring the
535 Molecular Mechanisms of Noncoding Alzheimer's Disease-Associated Genetic Variants. *Journal of*
536 *Alzheimer's Disease: JAD*, *72*(1), 301–318. https://doi.org/10.3233/JAD-190568
537 Asghari, K., Niknam, Z., Mohammadpour-Asl, S., & Chodari, L. (2024). Cellular junction dynamics and
538 Alzheimer's disease: A comprehensive review. *Molecular Biology Reports*, *51*(1), 273.
539 https://doi.org/10.1007/s11033-024-09242-w
540 Bao, M., Hanabuchi, S., Facchinetti, V., Du, Q., Bover, L., Plumas, J., Chaperot, L., Cao, W., Qin, J., Sun, S.-C.,
541 & Liu, Y.-J. (2012). CD2AP/SHIP1 complex positively regulates plasmacytoid dendritic cell receptor
542 signaling by inhibiting the E3 ubiquitin ligase Cbl. *Journal of Immunology (Baltimore, Md.: 1950)*,
543 *189*(2), 786–792. https://doi.org/10.4049/jimmunol.1200887

544 Behl, T., Kaur, D., Sehgal, A., Singh, S., Makeen, H. A., Albratty, M., Abdellatif, A. A. H., Dachani, S. R., &
545 Bungau, S. (2022). Exploring the potential role of rab5 protein in endo-lysosomal impairment in
546 Alzheimer's disease. *Biomedicine & Pharmacotherapy = Biomedecine & Pharmacotherapie*, *148*,
547 112773. https://doi.org/10.1016/j.biopha.2022.112773
548 Bettcher, B. M., Tansey, M. G., Dorothée, G., & Heneka, M. T. (2021). Peripheral and central immune
549 system crosstalk in Alzheimer disease—A research prospectus. *Nature Reviews Neurology*, *17*(11),
550 Article 11. https://doi.org/10.1038/s41582-021-00549-x
551 Cochran, J. N., Rush, T., Buckingham, S. C., & Roberson, E. D. (2015). The Alzheimer's disease risk factor
552 CD2AP maintains blood–brain barrier integrity. *Human Molecular Genetics*, *24*(23), 6667–6674.
553 https://doi.org/10.1093/hmg/ddv371
554 Cooper, J. D., Salehi, A., Delcroix, J. D., Howe, C. L., Belichenko, P. V., Chua-Couzens, J., Kilbridge, J. F.,
555 Carlson, E. J., Epstein, C. J., & Mobley, W. C. (2001). Failed retrograde transport of NGF in a mouse
556 model of Down's syndrome: Reversal of cholinergic neurodegenerative phenotypes following NGF
557 infusion. *Proceedings of the National Academy of Sciences of the United States of America*, *98*(18),
558 10439–10444. https://doi.org/10.1073/pnas.181219298
559 Cormont, M., Metón, I., Mari, M., Monzo, P., Keslair, F., Gaskin, C., McGraw, T. E., & Le Marchand-Brustel,
560 Y. (2003a). CD2AP/CMS regulates endosome morphology and traffic to the degradative pathway
561 through its interaction with Rab4 and c-Cbl. *Traffic (Copenhagen, Denmark)*, *4*(2), 97–112.
562 https://doi.org/10.1034/j.1600-0854.2003.40205.x
563 Cormont, M., Metón, I., Mari, M., Monzo, P., Keslair, F., Gaskin, C., McGraw, T. E., & Le Marchand-Brustel,
564 Y. (2003b). CD2AP/CMS regulates endosome morphology and traffic to the degradative pathway
565 through its interaction with Rab4 and c-Cbl. *Traffic (Copenhagen, Denmark)*, *4*(2), 97–112.
566 https://doi.org/10.1034/j.1600-0854.2003.40205.x
567 Delcroix, J.-D., Valletta, J. S., Wu, C., Hunt, S. J., Kowal, A. S., & Mobley, W. C. (n.d.). *NGF Signaling in*
568 *Sensory Neurons: Evidence that Early Endosomes Carry NGF Retrograde Signals*.

569 Dickson, D. W., Yen, S.-H., Suzuki, K. I., Davies, P., Garcia, J. H., & Hirano, A. (1986). Ballooned neurons in
570 select neurodegenerative diseases contain phosphorylated neurofilament epitopes. *Acta*
571 *Neuropathologica*, *71*(3), 216–223. https://doi.org/10.1007/BF00688042
572 Dustin, M. L., Olszowy, M. W., Holdorf, A. D., Li, J., Bromley, S., Desai, N., Widder, P., Rosenberger, F., van
573 der Merwe, P. A., Allen, P. M., & Shaw, A. S. (1998). A novel adaptor protein orchestrates receptor
574 patterning and cytoskeletal polarity in T-cell contacts. *Cell*, *94*(5), 667–677.
575 https://doi.org/10.1016/s0092-8674(00)81608-6
576 Engelhardt, J. von, Eliava, M., Meyer, A. H., Rozov, A., & Monyer, H. (2007). Functional Characterization of
577 Intrinsic Cholinergic Interneurons in the Cortex. *Journal of Neuroscience*, *27*(21), 5633–5642.
578 https://doi.org/10.1523/JNEUROSCI.4647-06.2007
579 Furusawa, K., Takasugi, T., Chiu, Y.-W., Hori, Y., Tomita, T., Fukuda, M., & Hisanaga, S. (2019). CD2-
580 associated protein (CD2AP) overexpression accelerates amyloid precursor protein (APP) transfer
581 from early endosomes to the lysosomal degradation pathway. *Journal of Biological Chemistry*,
582 *294*(28), 10886–10899. https://doi.org/10.1074/jbc.RA118.005385
583 Gamage, R., Zaborszky, L., Münch, G., & Gyengesi, E. (2023). Evaluation of eGFP expression in the ChAT-
584 eGFP transgenic mouse brain. *BMC Neuroscience*, *24*(1), 4. https://doi.org/10.1186/s12868-023-
585 00773-9
586 Gao, S., Hao, J., Zhao, Y., Li, X., Wang, T., Han, Z., Sun, B., Sun, J., & Liu, G. (2022). An updated analysis of
587 the association between CD2-associated protein gene rs9349407 polymorphism and Alzheimer's
588 disease in Chinese population. *Frontiers in Neuroinformatics*, *16*, 1006164.
589 https://doi.org/10.3389/fninf.2022.1006164
590 Geula, C., Dunlop, S. R., Ayala, I., Kawles, A. S., Flanagan, M. E., Gefen, T., & Mesulam, M.-M. (2021). Basal
591 forebrain cholinergic system in the dementias: Vulnerability, resilience, and resistance. *Journal of*
592 *Neurochemistry*, *158*(6), 1394–1411. https://doi.org/10.1111/jnc.15471

593 Gockley, J., Montgomery, K. S., Poehlman, W. L., Wiley, J. C., Liu, Y., Gerasimov, E., Greenwood, A. K.,
594 Sieberts, S. K., Wingo, A. P., Wingo, T. S., Mangravite, L. M., & Logsdon, B. A. (2021). Multi-tissue
595 neocortical transcriptome-wide association study implicates 8 genes across 6 genomic loci in
596 Alzheimer's disease. *Genome Medicine*, *13*(1), 76. https://doi.org/10.1186/s13073-021-00890-2
597 Hamano, Y., Grunkemeyer, J. A., Sudhakar, A., Zeisberg, M., Cosgrove, D., Morello, R., Lee, B., Sugimoto,
598 H., & Kalluri, R. (2002). Determinants of Vascular Permeability in the Kidney Glomerulus *. *Journal*
599 *of Biological Chemistry*, *277*(34), 31154–31162. https://doi.org/10.1074/jbc.M204806200
600 Harrison, B. J., Venkat, G., Lamb, J. L., Hutson, T. H., Drury, C., Rau, K. K., Bunge, M. B., Mendell, L. M.,
601 Gage, F. H., Johnson, R. D., Hill, C. E., Rouchka, E. C., Moon, L. D. F., & Petruska, J. C. (2016). The
602 Adaptor Protein CD2AP Is a Coordinator of Neurotrophin Signaling-Mediated Axon Arbor
603 Plasticity. *Journal of Neuroscience*, *36*(15), 4259–4275. https://doi.org/10.1523/JNEUROSCI.2423-
604 15.2016
605 Heppner, F. L., Ransohoff, R. M., & Becher, B. (2015). Immune attack: The role of inflammation in
606 Alzheimer disease. *Nature Reviews Neuroscience*, *16*(6), Article 6.
607 https://doi.org/10.1038/nrn3880
608 Hoeller, D., Volarevic, S., & Dikic, I. (2005). Compartmentalization of growth factor receptor signalling.
609 *Current Opinion in Cell Biology*, *17*(2), 107–111. https://doi.org/10.1016/j.ceb.2005.01.001
610 Hollingworth, P., Harold, D., Sims, R., Gerrish, A., Lambert, J.-C., Carrasquillo, M. M., Abraham, R.,
611 Hamshere, M. L., Pahwa, J. S., Moskvina, V., Dowzell, K., Jones, N., Stretton, A., Thomas, C.,
612 Richards, A., Ivanov, D., Widdowson, C., Chapman, J., Lovestone, S., … Williams, J. (2011). Common
613 variants at ABCA7, MS4A6A/MS4A4E, EPHA1, CD33 and CD2AP are associated with Alzheimer's
614 disease. *Nature Genetics*, *43*(5), 429–435. https://doi.org/10.1038/ng.803
615 Howe, C. L., & Mobley, W. C. (2004). Signaling endosome hypothesis: A cellular mechanism for long
616 distance communication. *Journal of Neurobiology*, *58*(2), 207–216.
617 https://doi.org/10.1002/neu.10323

618 Iulita, M. F., & Cuello, A. C. (2016). The NGF Metabolic Pathway in the CNS and its Dysregulation in Down
619 Syndrome and Alzheimer's Disease. *Current Alzheimer Research*, *13*(1), 53–67.
620 https://doi.org/10.2174/1567205012666150921100030
621 Iwano, T., Sobajima, T., Takeda, S., Harada, A., & Yoshimura, S. (2023). The Rab GTPase-binding protein
622 EHBP1L1 and its interactors CD2AP/CIN85 negatively regulate the length of primary cilia via actin
623 remodeling. *Journal of Biological Chemistry*, *299*(3). https://doi.org/10.1016/j.jbc.2023.102985
624 Jung, H., Lee, Y., Lee, S.-H., & Sohn, J.-H. (2023). Auditory or Audiovisual Stimulation Ameliorates Cognitive
625 Impairment and Neuropathology in ApoE4 Knock-In Mice. *International Journal of Molecular*
626 *Sciences*, *24*(2), Article 2. https://doi.org/10.3390/ijms24020938
627 Kawabata, S. (2022). Signaling abnormality leading to excessive/aberrant synaptic plasticity in Alzheimer's
628 disease. *Frontiers in Aging Neuroscience*, *14*, 1062519.
629 https://doi.org/10.3389/fnagi.2022.1062519
630 Khaire, A. S., Wimberly, C. E., Semmes, E. C., Hurst, J. H., & Walsh, K. M. (2022). An integrated genome and
631 phenome-wide association study approach to understanding Alzheimer's disease predisposition.
632 *Neurobiology of Aging*, *118*, 117–123. https://doi.org/10.1016/j.neurobiolaging.2022.05.011
633 Kim, W., Underwood, R. S., Greenwald, I., & Shaye, D. D. (2018). OrthoList 2: A New Comparative Genomic
634 Analysis of Human and Caenorhabditis elegans Genes. *Genetics*, *210*(2), 445–461.
635 https://doi.org/10.1534/genetics.118.301307
636 Kirsch, K. H., Georgescu, M.-M., Shishido, T., Langdon, W. Y., Birge, R. B., & Hanafusa, H. (2001). The
637 Adapter Type Protein CMS/CD2AP Binds to the Proto-oncogenic Protein c-Cbl through a Tyrosine
638 Phosphorylation-regulated Src Homology 3 Domain Interaction*. *Journal of Biological Chemistry*,
639 *276*(7), 4957–4963. https://doi.org/10.1074/jbc.M005784200
640 Koizumi, K., Wang, G., & Park, L. (2016). Endothelial Dysfunction and Amyloid-β-Induced Neurovascular
641 Alterations. *Cellular and Molecular Neurobiology*, *36*(2), 155–165.
642 https://doi.org/10.1007/s10571-015-0256-9

643 Kovacs, G. G., Robinson, J. L., Xie, S. X., Lee, E. B., Grossman, M., Wolk, D. A., Irwin, D. J., Weintraub, D.,
644 Kim, C. F., Schuck, T., Yousef, A., Wagner, S. T., Suh, E., Van Deerlin, V. M., Lee, V. M.-Y., &
645 Trojanowski, J. Q. (2017). Evaluating the Patterns of Aging-Related Tau Astrogliopathy Unravels
646 Novel Insights Into Brain Aging and Neurodegenerative Diseases. *Journal of Neuropathology &*
647 *Experimental Neurology*, *76*(4), 270–288. https://doi.org/10.1093/jnen/nlx007
648 Kunkle, B. W., Schmidt, M., Klein, H.-U., Naj, A. C., Hamilton-Nelson, K. L., Larson, E. B., Evans, D. A., De
649 Jager, P. L., Crane, P. K., Buxbaum, J. D., Ertekin-Taner, N., Barnes, L. L., Fallin, M. D., Manly, J. J.,
650 Go, R. C. P., Obisesan, T. O., Kamboh, M. I., Bennett, D. A., Hall, K. S., … Kukull, W. A. (2021). Novel
651 Alzheimer Disease Risk Loci and Pathways in African American Individuals Using the African
652 Genome Resources Panel: A Meta-analysis. *JAMA Neurology*, *78*(1), 102.
653 https://doi.org/10.1001/jamaneurol.2020.3536
654 Lambert, J. C., Ibrahim-Verbaas, C. A., Harold, D., Naj, A. C., Sims, R., Bellenguez, C., DeStafano, A. L., Bis, J.
655 C., Beecham, G. W., Grenier-Boley, B., Russo, G., Thorton-Wells, T. A., Jones, N., Smith, A. V.,
656 Chouraki, V., Thomas, C., Ikram, M. A., Zelenika, D., Vardarajan, B. N., … Amouyel, P. (2013). Meta-
657 analysis of 74,046 individuals identifies 11 new susceptibility loci for Alzheimer's disease. *Nature*
658 *Genetics*, *45*(12), 1452–1458. https://doi.org/10.1038/ng.2802
659 Latina, V., Atlante, A., Malerba, F., La Regina, F., Balzamino, B. O., Micera, A., Pignataro, A., Stigliano, E.,
660 Cavallaro, S., Calissano, P., & Amadoro, G. (2023). The Cleavage-Specific Tau 12A12mAb Exerts an
661 Anti-Amyloidogenic Action by Modulating the Endocytic and Bioenergetic Pathways in Alzheimer's
662 Disease Mouse Model. *International Journal of Molecular Sciences*, *24*(11), Article 11.
663 https://doi.org/10.3390/ijms24119683
664 Lehtonen, S., Tienari, J., Londesborough, A., Pirvola, U., Ora, A., Reima, I., & Lehtonen, E. (2008). CD2-
665 associated protein is widely expressed and differentially regulated during embryonic
666 development. *Differentiation*, *76*(5), 506–517. https://doi.org/10.1111/j.1432-0436.2007.00255.x

667 Li, C., Ruotsalainen, V., Tryggvason, K., Shaw, A. S., & Miner, J. H. (2000). CD2AP is expressed with nephrin
668 in developing podocytes and is found widely in mature kidney and elsewhere. *American Journal of*
669 *Physiology. Renal Physiology*, *279*(4), F785-792. https://doi.org/10.1152/ajprenal.2000.279.4.F785
670 Liu, R., Collier, J. M., Abdul-Rahman, N.-H., Capuk, O., Zhang, Z., & Begum, G. (2024). Dysregulation of Ion
671 Channels and Transporters and Blood-Brain Barrier Dysfunction in Alzheimer's Disease and
672 Vascular Dementia. *Aging and Disease*. https://doi.org/10.14336/AD.2023.1201
673 Maninger, J.-K., Nowak, K., Goberdhan, S., O'Donoghue, R., & Connor-Robson, N. (2024). Cell type-specific
674 functions of Alzheimer's disease endocytic risk genes. *Philosophical Transactions of the Royal*
675 *Society B: Biological Sciences*, *379*(1899), 20220378. https://doi.org/10.1098/rstb.2022.0378
676 Marioni, R. E., Harris, S. E., Zhang, Q., McRae, A. F., Hagenaars, S. P., Hill, W. D., Davies, G., Ritchie, C. W.,
677 Gale, C. R., Starr, J. M., Goate, A. M., Porteous, D. J., Yang, J., Evans, K. L., Deary, I. J., Wray, N. R.,
678 & Visscher, P. M. (2018). GWAS on family history of Alzheimer's disease. *Translational Psychiatry*,
679 *8*(1), Article 1. https://doi.org/10.1038/s41398-018-0150-6
680 Naj, A. C., Jun, G., Beecham, G. W., Wang, L.-S., Vardarajan, B. N., Buros, J., Gallins, P. J., Buxbaum, J. D.,
681 Jarvik, G. P., Crane, P. K., Larson, E. B., Bird, T. D., Boeve, B. F., Graff-Radford, N. R., De Jager, P. L.,
682 Evans, D., Schneider, J. A., Carrasquillo, M. M., Ertekin-Taner, N., … Schellenberg, G. D. (2011).
683 Common variants at MS4A4/MS4A6E, CD2AP, CD33 and EPHA1 are associated with late-onset
684 Alzheimer's disease. *Nature Genetics*, *43*(5), 436–441. https://doi.org/10.1038/ng.801
685 Nakagawa, T., Hasegawa, Y., Uekawa, K., & Kim-Mitsuyama, S. (2017). Chronic kidney disease accelerates
686 cognitive impairment in a mouse model of Alzheimer's disease, through angiotensin II.
687 *Experimental Gerontology*, *87*, 108–112. https://doi.org/10.1016/j.exger.2016.11.012
688 Nisbet, R. M., Polanco, J.-C., Ittner, L. M., & Götz, J. (2015). Tau aggregation and its interplay with amyloid-
689 β. *Acta Neuropathologica*, *129*(2), 207–220. https://doi.org/10.1007/s00401-014-1371-2
690 Novikova, G., Kapoor, M., Tcw, J., Abud, E. M., Efthymiou, A. G., Chen, S. X., Cheng, H., Fullard, J. F., Bendl,
691 J., Liu, Y., Roussos, P., Björkegren, J. L., Liu, Y., Poon, W. W., Hao, K., Marcora, E., & Goate, A. M.

692 (2021). Integration of Alzheimer's disease genetics and myeloid genomics identifies disease risk
693 regulatory elements and genes. *Nature Communications*, *12*(1), Article 1.
694 https://doi.org/10.1038/s41467-021-21823-y
695 Ojelade, S. A., Lee, T. V., Giagtzoglou, N., Yu, L., Ugur, B., Li, Y., Duraine, L., Zuo, Z., Petyuk, V., De Jager, P.
696 L., Bennett, D. A., Arenkiel, B. R., Bellen, H. J., & Shulman, J. M. (2019). Cindr, the Drosophila
697 Homolog of the CD2AP Alzheimer's Disease Risk Gene, Is Required for Synaptic Transmission and
698 Proteostasis. *Cell Reports*, *28*(7), 1799-1813.e5. https://doi.org/10.1016/j.celrep.2019.07.041
699 Pandey, R. S., Kotredes, K. P., Sasner, M., Howell, G. R., & Carter, G. W. (2023). Differential splicing of
700 neuronal genes in a Trem2*R47H mouse model mimics alterations associated with Alzheimer's
701 disease. *BMC Genomics*, *24*(1), 172. https://doi.org/10.1186/s12864-023-09280-x
702 Pensalfini, A., Kim, S., Subbanna, S., Bleiwas, C., Goulbourne, C. N., Stavrides, P. H., Jiang, Y., Lee, J.-H.,
703 Darji, S., Pawlik, M., Huo, C., Peddy, J., Berg, M. J., Smiley, J. F., Basavarajappa, B. S., & Nixon, R. A.
704 (2020). Endosomal Dysfunction Induced by Directly Overactivating Rab5 Recapitulates Prodromal
705 and Neurodegenerative Features of Alzheimer's Disease. *Cell Reports*, *33*(8), 108420.
706 https://doi.org/10.1016/j.celrep.2020.108420
707 Qui, M. S., & Green, S. H. (1992). PC12 cell neuronal differentiation is associated with prolonged p21ras
708 activity and consequent prolonged ERK activity. *Neuron*, *9*(4), 705–717.
709 https://doi.org/10.1016/0896-6273(92)90033-a
710 Rajabli, F., Benchek, P., Tosto, G., Kushch, N., Sha, J., Bazemore, K., Zhu, C., Lee, W.-P., Haut, J., Hamilton-
711 Nelson, K. L., Wheeler, N. R., Zhao, Y., Farrell, J. J., Grunin, M. A., Leung, Y. Y., Kuksa, P. P., Li, D.,
712 Lucio da Fonseca, E., Mez, J. B., … Naj, A. C. (2023). Multi-ancestry genome-wide meta-analysis of
713 56,241 individuals identifies LRRC4C, LHX5-AS1 and nominates ancestry-specific loci PTPRK ,
714 GRB14 , and KIAA0825 as novel risk loci for Alzheimer's disease: The Alzheimer's Disease Genetics
715 Consortium. *medRxiv: The Preprint Server for Health Sciences*, 2023.07.06.23292311.
716 https://doi.org/10.1101/2023.07.06.23292311

717 Renier, N., Wu, Z., Simon, D. J., Yang, J., Ariel, P., & Tessier-Lavigne, M. (2014). iDISCO: A Simple, Rapid
718 Method to Immunolabel Large Tissue Samples for Volume Imaging. *Cell*, *159*(4), 896–910.
719 https://doi.org/10.1016/j.cell.2014.10.010
720 Rouka, E., Simister, P. C., Janning, M., Kumbrink, J., Konstantinou, T., Muniz, J. R. C., Joshi, D., O'Reilly, N.,
721 Volkmer, R., Ritter, B., Knapp, S., von Delft, F., Kirsch, K. H., & Feller, S. M. (2015). Differential
722 Recognition Preferences of the Three Src Homology 3 (SH3) Domains from the Adaptor CD2-
723 associated Protein (CD2AP) and Direct Association with Ras and Rab Interactor 3 (RIN3). *The*
724 *Journal of Biological Chemistry*, *290*(42), 25275–25292. https://doi.org/10.1074/jbc.M115.637207
725 Rueden, C. T., Schindelin, J., Hiner, M. C., DeZonia, B. E., Walter, A. E., Arena, E. T., & Eliceiri, K. W. (2017).
726 ImageJ2: ImageJ for the next generation of scientific image data. *BMC Bioinformatics*, *18*(1), 529.
727 https://doi.org/10.1186/s12859-017-1934-z
728 Sang, Q., Sun, D., Chen, Z., & Zhao, W. (2018). NGF and PI3K/Akt signaling participate in the ventral motor
729 neuronal protection of curcumin in sciatic nerve injury rat models. *Biomedicine &*
730 *Pharmacotherapy*, *103*, 1146–1153. https://doi.org/10.1016/j.biopha.2018.04.116
731 Saunders, A., Macosko, E. Z., Wysoker, A., Goldman, M., Krienen, F. M., de Rivera, H., Bien, E., Baum, M.,
732 Bortolin, L., Wang, S., Goeva, A., Nemesh, J., Kamitaki, N., Brumbaugh, S., Kulp, D., & McCarroll, S.
733 A. (2018). Molecular Diversity and Specializations among the Cells of the Adult Mouse Brain. *Cell*,
734 *174*(4), 1015-1030.e16. https://doi.org/10.1016/j.cell.2018.07.028
735 Schaefer, A., van Duijn, T. J., Majolee, J., Burridge, K., & Hordijk, P. L. (2017). Endothelial CD2AP Binds the
736 Receptor ICAM-1 To Control Mechanosignaling, Leukocyte Adhesion, and the Route of Leukocyte
737 Diapedesis In Vitro. *The Journal of Immunology*, *198*(12), 4823–4836.
738 https://doi.org/10.4049/jimmunol.1601987
739 Schwarz, K., Simons, M., Reiser, J., Saleem, M. A., Faul, C., Kriz, W., Shaw, A. S., Holzman, L. B., & Mundel,
740 P. (2001, December 1). *Podocin, a raft-associated component of the glomerular slit diaphragm,*

741 *interacts with CD2AP and nephrin*. American Society for Clinical Investigation.
742 https://doi.org/10.1172/JCI12849
743 Shen, R., Zhao, X., He, L., Ding, Y., Xu, W., Lin, S., Fang, S., Yang, W., Sung, K., Spencer, B., Rissman, R. A.,
744 Lei, M., Ding, J., & Wu, C. (2020). Upregulation of RIN3 induces endosomal dysfunction in
745 Alzheimer's disease. *Translational Neurodegeneration*, *9*(1), 26. https://doi.org/10.1186/s40035-
746 020-00206-1
747 Sherva, R., Zhang, R., Sahelijo, N., Jun, G., Anglin, T., Chanfreau, C., Cho, K., Fonda, J. R., Gaziano, J. M.,
748 Harrington, K. M., Ho, Y.-L., Kremen, W. S., Litkowski, E., Lynch, J., Neale, Z., Roussos, P., Marra, D.,
749 Mez, J., Miller, M. W., … Logue, M. W. (2023). African ancestry GWAS of dementia in a large
750 military cohort identifies significant risk loci. *Molecular Psychiatry*, *28*(3), 1293–1302.
751 https://doi.org/10.1038/s41380-022-01890-3
752 Shi, Y., Liu, Z., Shen, Y., & Zhu, H. (2018). A Novel Perspective Linkage Between Kidney Function and
753 Alzheimer's Disease. *Frontiers in Cellular Neuroscience*, *12*.
754 https://www.frontiersin.org/articles/10.3389/fncel.2018.00384
755 Shih, N. Y., Li, J., Karpitskii, V., Nguyen, A., Dustin, M. L., Kanagawa, O., Miner, J. H., & Shaw, A. S. (1999).
756 Congenital nephrotic syndrome in mice lacking CD2-associated protein. *Science (New York, N.Y.)*,
757 *286*(5438), 312–315. https://doi.org/10.1126/science.286.5438.312
758 Shulman, J. M., Imboywa, S., Giagtzoglou, N., Powers, M. P., Hu, Y., Devenport, D., Chipendo, P., Chibnik, L.
759 B., Diamond, A., Perrimon, N., Brown, N. H., De Jager, P. L., & Feany, M. B. (2014). Functional
760 screening in Drosophila identifies Alzheimer's disease susceptibility genes and implicates Tau-
761 mediated mechanisms. *Human Molecular Genetics*, *23*(4), 870–877.
762 https://doi.org/10.1093/hmg/ddt478
763 Srivatsan, S., Swiecki, M., Otero, K., Cella, M., & Shaw, A. S. (2013). CD2-Associated Protein Regulates
764 Plasmacytoid Dendritic Cell Migration, but Is Dispensable for Their Development and Cytokine

765 Production. *The Journal of Immunology*, *191*(12), 5933–5940.
766 https://doi.org/10.4049/jimmunol.1300454
767 Stauffer, W., Sheng, H., & Lim, H. N. (2018). EzColocalization: An ImageJ plugin for visualizing and
768 measuring colocalization in cells and organisms. *Scientific Reports*, *8*(1), Article 1.
769 https://doi.org/10.1038/s41598-018-33592-8
770 Tallini, Y. N., Shui, B., Greene, K. S., Deng, K.-Y., Doran, R., Fisher, P. J., Zipfel, W., & Kotlikoff, M. I. (2006).
771 BAC transgenic mice express enhanced green fluorescent protein in central and peripheral
772 cholinergic neurons. *Physiological Genomics*, *27*(3), 391–397.
773 https://doi.org/10.1152/physiolgenomics.00092.2006
774 Tesi, N., van der Lee, S. J., Hulsman, M., Jansen, I. E., Stringa, N., van Schoor, N. M., Scheltens, P., van der
775 Flier, W. M., Huisman, M., Reinders, M. J. T., & Holstege, H. (2020). Immune response and
776 endocytosis pathways are associated with the resilience against Alzheimer's disease. *Translational*
777 *Psychiatry*, *10*(1), Article 1. https://doi.org/10.1038/s41398-020-01018-7
778 Tsui, C. C., & Pierchala, B. A. (2008). CD2AP and Cbl-3/Cbl-c Constitute a Critical Checkpoint in the
779 Regulation of Ret Signal Transduction. *Journal of Neuroscience*, *28*(35), 8789–8800.
780 https://doi.org/10.1523/JNEUROSCI.2738-08.2008
781 van Bree, E. J., Guimarães, R. L. F. P., Lundberg, M., Blujdea, E. R., Rosenkrantz, J. L., White, F. T. G.,
782 Poppinga, J., Ferrer-Raventós, P., Schneider, A.-F. E., Clayton, I., Haussler, D., Reinders, M. J. T.,
783 Holstege, H., Ewing, A. D., Moses, C., & Jacobs, F. M. J. (2022). A hidden layer of structural
784 variation in transposable elements reveals potential genetic modifiers in human disease-risk loci.
785 *Genome Research*, *32*(4), 656–670. https://doi.org/10.1101/gr.275515.121
786 Vandal, M., Institoris, A., Korin, B., Gunn, C., Lee, S., Lee, J., Bourassa, P., Mishra, R. C., Peringod, G., Jiang,
787 Y., Hirai, S., Belzil, C., Reveret, L., Tremblay, C., Hashem, M., Elias, E., Meilandt, B., Foreman, O.,
788 Rouse-Girma, M., … Nguyen, M. D. (2022). *The Alzheimer risk factor CD2AP causes dysfunction of*

789 *the brain vascular network* (p. 2020.12.10.419598). bioRxiv.
790 https://doi.org/10.1101/2020.12.10.419598
791 Welsch, T., Endlich, N., Gökce, G., Doroshenko, E., Simpson, J. C., Kriz, W., Shaw, A. S., & Endlich, K. (2005).
792 Association of CD2AP with dynamic actin on vesicles in podocytes. *American Journal of Physiology.*
793 *Renal Physiology*, *289*(5), F1134-1143. https://doi.org/10.1152/ajprenal.00178.2005
794 Welsch, T., Endlich, N., Kriz, W., & Endlich, K. (2001). CD2AP and p130Cas localize to different F-actin
795 structures in podocytes. *American Journal of Physiology-Renal Physiology*, *281*(4), F769–F777.
796 https://doi.org/10.1152/ajprenal.2001.281.4.F769
797 Wittmann, C. W., Wszolek, M. F., Shulman, J. M., Salvaterra, P. M., Lewis, J., Hutton, M., & Feany, M. B.
798 (2001). Tauopathy in Drosophila: Neurodegeneration Without Neurofibrillary Tangles. *Science*,
799 *293*(5530), 711–714. https://doi.org/10.1126/science.1062382
800 Xu, W., Fang, F., Ding, J., & Wu, C. (2018a). Dysregulation of Rab5-mediated endocytic pathways in
801 Alzheimer's disease. *Traffic*, *19*(4), 253–262. https://doi.org/10.1111/tra.12547
802 Xu, W., Fang, F., Ding, J., & Wu, C. (2018b). Dysregulation of Rab5-mediated endocytic pathways in
803 Alzheimer's disease. *Traffic (Copenhagen, Denmark)*, *19*(4), 253–262.
804 https://doi.org/10.1111/tra.12547
805 Xue, Y.-Y., Chen, Y.-H., Lin, R.-R., Huang, H.-F., Wu, Z.-Y., & Tao, Q.-Q. (2022). Alzheimer's disease
806 susceptibility locus in CD2AP is associated with increased cerebrospinal fluid tau levels in mild
807 cognitive impairment. *Neuroscience Letters*, *771*, 136419.
808 https://doi.org/10.1016/j.neulet.2021.136419
809 Ye, H., Kuruvilla, R., Zweifel, L. S., & Ginty, D. D. (2003). Evidence in Support of Signaling Endosome-Based
810 Retrograde Survival of Sympathetic Neurons. *Neuron*, *39*(1), 57–68.
811 https://doi.org/10.1016/S0896-6273(03)00266-6
812 Yoshida, S., Wei, X., Zhang, G., O'Connor, C. L., Torres, M., Zhou, Z., Lin, L., Menon, R., Xu, X., Zheng, W.,
813 Xiong, Y., Otto, E., Tang, C.-H. A., Hua, R., Verma, R., Mori, H., Zhang, Y., Hu, C.-C. A., Liu, M., … Qi,

814 L. (2021, April 1). *Endoplasmic reticulum–associated degradation is required for nephrin*
815 *maturation and kidney glomerular filtration function*. American Society for Clinical Investigation.
816 https://doi.org/10.1172/JCI143988
817 Zhang, C.-Y., He, F.-F., Su, H., Zhang, C., & Meng, X.-F. (2020). Association between chronic kidney disease
818 and Alzheimer's disease: An update. *Metabolic Brain Disease*, *35*(6), 883–894.
819 https://doi.org/10.1007/s11011-020-00561-y

820

821

822 **FIGURE LEGENDS**

823

824 **FIGURE 1**

825 CD2AP mRNA is expressed in Ntrk1 (TRKA)-expressing populations of cholinergic neurons of the
826 adult mouse brain. Summary of single-cell RNA-sequencing data from the adult mouse brain,
827 using the Dropviz webtool (Saunders et al., 2018). The top ten, highest *CD2AP*-expressing
828 populations are shown on the left (magenta) and corresponding expression levels of *Ntrk1* on the
829 right (cyan).

830

831 **FIGURE 2**

832 CD2AP protein is expressed in ChAT-positive neurons in vivo. (a) Representative confocal image
833 of ChAT-GFP mouse brain 20um section, stained with primary antibodies to ChAT (yellow) and
834 Cd2ap (magenta). (b) Inset indicated by yellow square; diagonal band of broca (vDB). CD2AP
835 signal is delectated in adult (ChAT-GFP+/ChAT-antibody+) cholinergic neurons.

836

837 **FIGURE 3**

838 Immunofluorescence analysis of ChAT-GFP neurons in regions of interest within the mouse brain.
839 Representative immunofluorescence images from 20um-thick frozen tissue sections. ChAT-GFP
840 signal (left column, cyan) was detected in ChAT-lineage neurons (ChAT-GFP+/αChAT-) in Cortex
841 (top row), Striatum, Brocca (vDB) and Substantia Innominata (bottom row). Fluorescence signal
842 from α (second column, yellow) was observed in neuron soma of adult (ChAT-GFP+/ αChAT+)
843 cholinergic neurons in Striatum (second row), Brocca (third row) and Substantia Innominata
844 (bottom row). Fluorescence signal of CD2AP (third column, magenta), was observed in adult
845 cholinergic neurons (ChAT-GFP+/ αChAT+), but not in cholinergic-lineage neurons (ChAT-
846 GFP+/αChAT-). Cyan arrows indicate ChAT-GFP+/αChAT- neuron cell bodies; magenta arrows
847 indicate (cortical) vascular αCD2AP; white arrows indicate ChAT-GFP+/ αChAT+ neuron cell
848 bodies that are also CD2AP+.

849

850 **FIGURE 4**

851 Quantification of CD2AP protein expression in cholinergic neurons. (a) Mean, regional expression
852 levels (expressed as integrated density mean ± SD) of Cd2ap in individual mice; violin clusters
853 reflect raw data point distribution and mean values ± SD. (b) Mean CD2AP immunofluorescence
854 signals in ChAT-GFP+ soma from indicated brain regions, from group data (N=3 animals). One-
855 way analysis of variance (ANOVA) with Tukey post-hoc analysis revealed Cd2ap expression in
856 the basal, striatal and optic regions of the mouse brain, with cortex serving as a background-
857 signal control. ****$p<0.0001$.

858

859 **FIGURE 5**

860 CD2AP expression in ChAT-GFP+ adult mouse brain projections. (a) Representative, whole-brain
861 imaging of ChAT-GFP+, sagittal sections (150um) embedded in agarose. (a; i) ChAT/GFP+

862 cholinergic neuron cell bodies originating in the basal forebrain; (a; ii) ChAT/GFP+ axonal
863 projections (white arrow) from basal forebrain on trajectory towards hippocampal/iso-cortical
864 regions. (b-c) Representative, regional examination of Cd2ap expression with
865 immunofluorescence analysis of ChAT-GFP+ neuron cell bodies in the basal forebrain (b; white
866 arrows) and staining patterning consistent with ChAT/GFP+ axonal projections (a; i, ii). Yellow box
867 indicates low magnification location of inset image at high magnification; cyan indicates
868 endogenous ChAT/GFP+ fluorescence signal; magenta indicates fluorescence signal from anti-
869 Cd2ap primary antibody; white arrows indicate areas of overlap between ChAT/GFP+ and
870 Cd2ap+.

871

872

873 **FIGURE 6**

874 CD2AP and Rab5 co-expression in ChAT/GFP-positive (ChAT/GFP+) neurons in adult mouse
875 brains (aged 10 months). (a) Representative immunofluorescence image from the vDB region
876 (Basal forebrain; 20um), demonstrating the colocalization and co-expression of CD2AP and Rab5
877 endosomal formations within and in proximity to cell bodies of ChAT/GFP+ cholinergic neurons.
878 White arrows indicate punctate endosomal formations localizing around/within the ChAT/GFP+
879 cell body. (b, top) Representative region of interest (ROI) outlined in cyan, indicating the outline of
880 a single, ChAT/GFP+ neuron cell body; area within ROI is the max projection of colocalized
881 Cd2ap/Rab5+ endosomes, a single example of which is indicated with a red arrow and circle. (b,
882 bottom) Representative, two-dimensional intensity histogram demonstrating the quantification
883 (correlation) of Cd2ap/Rab5+ endosomes.

TABLE 1. Antibodies used.

Primary Antibody	Source	Cat#	Lot#	Species/clonality	[working] IHC/IF (20um)	[working] IHC/IF (150um)
Anti-Cd2ap	Proteintech	51046-1-AP	23812	Rabbit polyclonal (IgG)	1:800	1:200
Anti-TrkA (Rat)	R&D	AF1056	VFA0118091	Goat polyclonal (IgG)	1:200	1:100
Anti-Choline Acetyltransferase (ChAT)	Millipore/Sigma	AB144P	3926290	Goat polyclonal (IgG)	1:200	1:100
Anti-Green Fluorescence Protein	Aves Labs	GFP-1020	GFP917979	Chicken (IgY)	1:1000	(1:500)10mg/mL
Anti-Rab5	Cell Signaling Technology	46449	3	Mouse monoclonal (IgG1; clone E6N8S)	1:200	N/A
Secondary Antibody/fluorophore	**Source**	**Cat#**	**Lot#**	**Species**	**[working] IHC/IF (20um)**	**[working] IHC/IF (150um)**
Alexa647	Jackson ImmunoResearch	711-605-152	165592	Donkey-Anti-Rabbit	1:500	1:250
Cy3		705-165-147	130439	Donkey-Anti-Goat	1:500	1:250
Alexa488		703-545-155	139424	Donkey-Anti-Chicken	N/A	1:250
Cy3		705-165-147	130439	Donkey-Anti-Goat	N/A	1:250
Alexa647		703-605-155	138591	Donkey-Anti-Chicken	N/A	1:250
Cy3		711-165-152	166393	Donkey-Anti-Rabbit	N/A	1:250
Alexa647		705-605-147	160039	Donkey-Anti-Goat	1:500	N/A
Cy3		715-165-151	130991	Donkey-Anti-Mouse	1:500	N/A
Alexa488		711-545-152	161527	Donkey-Anti-Rabbit	1:500	N/A
Other Reagents	**Source**	**Cat#**	**Lot#**	**Species**	**[working] IHC/IF (20um)**	**[working] IHC/IF (150um)**
Normal Donkey Serum	Jackson ImmunoResearch	167385	017-000-121	4%	8%	017-000-121
Mounting Medium with DAPI	Abcam	ab104139	1043154-3	n/a	n/a	ab104139

TABLE 2. Summary of GWAS studies from 2013 to present (June 2024) implicating Cd2ap in the pathogenesis and/or susceptibility to AD in humans.

YEAR	CITATION	OUTCOME	rsID
2023	Sherva R, Zhang R, Sahelijo N, et al. African ancestry GWAS of dementia in a large military cohort identifies significant risk loci. Mol Psychiatry. 2023;28(3):1293-1302.	Novel, significant SNPs near known AD risk genes TREM2, CD2AP, and ABCA7; peak variants in these genes differed from those previously reported in European and African ancestry cohorts.	rs7738720
2023	Charisis S, Lin H, Ray R, et al. Obesity impacts the expression of Alzheimer's disease-related genes: The Framingham Heart Study. Alzheimers Dement. 2023;19(8):3496-3505.	Gene expression was measured for 74 AD-related genes, derived by integrating genome-wide association study results with functional genomics data from the Framingham Heart Study. Obesity metrics were associated with the expression of 21 AD-related genes. The strongest associations were observed with CLU, CD2AP, KLC3, and FCER1G.	
2022	Gao S, Hao JW, Zhao YN, et al. An updated analysis of the association between CD2-associated protein gene rs9349407 polymorphism and Alzheimer's disease in Chinese population. Front Neuroinform. 2022;16:1006164.	Comparison of 11 independent studies from 8 articles exploring the correlation between rs9349407 variation and AD in Chinese. Additional meta-analysis based on fixed and random effect models were compiled to perform heterogeneity test. Use of additive model, dominant model, and recessive model for subgroup analysis demonstrated that the CD2AP rs9349407 polymorphism increases AD susceptibility in Chinese populations.	rs9349407
2022	Khaire AS, Wimberly CE, Semmes EC, Hurst JH, Walsh KM. An integrated genome and phenome-wide association study approach to understanding Alzheimer's disease predisposition. Neurobiol Aging. 2022;118:117-123.	“Phenome-wide association” of 23 known, LOAD-associated SNPs and 4:1 matched control SNPs using UK Biobank data; associations confirmed known LOAD risk loci near PICALM, CD2AP, SPI1, and NDUFAF6, and identified a novel risk locus in epidermal growth factor receptor.	
2022	Bellenguez, C., Küçükali, F., Jansen, I.E. et al. New insights into the genetic etiology of Alzheimer’s disease and related dementias. Nat Genet 2022; 54:412–436	Two-stage GWAS of 111,326 clinically diagnosed/‘proxy’ AD cases and 677,663 controls; found 75 risk loci, including 42 novel sites at the time of analysis. Pathway enrichment analyses confirmed involvement of amyloid/tau pathways and highlighted microglia implication.	rs7767350 6:47517390:T:C
2021	Li Y, Laws SM, Miles LA, et al. Genomics of Alzheimer's disease implicates the innate and adaptive immune systems. Cell Mol Life Sci. 2021;78(23):7397-7426.	Comprehensive review of GWAS studies (with meta-analyses from 2013 up to 2021)	
2021	Kunkle BW, Schmidt M, Klein HU, et al. Novel Alzheimer Disease Risk Loci and Pathways in African American Individuals Using the African Genome Resources Panel: A Meta-analysis. JAMA Neurol. 2021;78(1):102-113.	Of 25 known AD loci in non-Hispanic, White individuals, only APOE, ABCA7, TREM2, BIN1, CD2AP, FERMT2, and WWOX were significantly associated with AD in African American individuals.	
2021	Schwartzentruber J, Cooper S, Liu JZ, Barrio-Hernandez I, Bello E, Kumasaka N et al. Genome-wide meta-analysis, fine-mapping and integrative prioritization implicate new Alzheimer’s disease risk genes. Nat Genet 2021:53(3):392–402.	AD GWAS with focus on causal genes and variants; confirmed recently discovered AD genes (CD2AP) also the top gene within 500 kb by network score and AD Risk.	rs9381563 6:47432637:C:T
2019	Jansen IE, Savage JE, Watanabe K, Bryois J, Williams DM, Steinberg S et al. Genome-wide meta-analysis identifies new loci and functional pathways influencing Alzheimer’s disease risk. Nat Genet 2019:51(3):404–413.	AD GWAS of clinically diagnosed AD and AD-by-proxy cases; meta-analysis results revealed 29 risk loci, implicating 215 potential causative genes (CD2AP); analyses support a role for lipid processing and degradation of amyloid precursor proteins in AD pathogenesis.	rs9381563 6:47432637:C:T
2019	Kunkle BW, Grenier-Boley B, Sims R, Bis JC, Damotte V, Naj AC et al. Genetic meta-analysis of diagnosed Alzheimer’s disease identifies new risk loci and implicates Abeta, tau, immunity and lipid processing. Nat Genet 2019;51(3):414–430.	AD GWAS; confirmed eQTLs for genes in previously identified loci, including *CD2AP* and the *CD2AP* locus	rs9473117 6:47431284:A:C
2018	Marioni, R.E., Harris, S.E., Zhang, Q. et al. GWAS on family history of Alzheimer’s disease. Transl Psychiatry 2018; 8, 99.	Self-report of parental history of Alzheimer’s dementia for GWAS of 314,278 participants from UK Biobank; meta-analysis with published consortium data revealed three new loci, relevant for AD and neurodegeneration, including CD2AP.	rs9381563 6:47432637:C:T
2013	Lambert JC, Ibrahim-Verbaas CA, Harold D, Naj AC, Sims R, Bellenguez C et al. Meta-analysis of 74,046 individuals identifies 11 new susceptibility loci for Alzheimer’s disease. Nat Genet 2013; 45(12):1452–1458.	Meta-analysis of 17,008 cases and 37,154 controls, followed by replication in an independent cohort; confirmed previous GWAS findings (CD2AP) and identified 11 novel AD susceptibility loci: HLA-DRB5-DRB1, SORL1, PTK2B, SLC24A4, ZCWPW1, CELF1, NME8, FERMT2, CASS4, INPP5D, and MEF2C	rs10948363 6:47487762:A:G

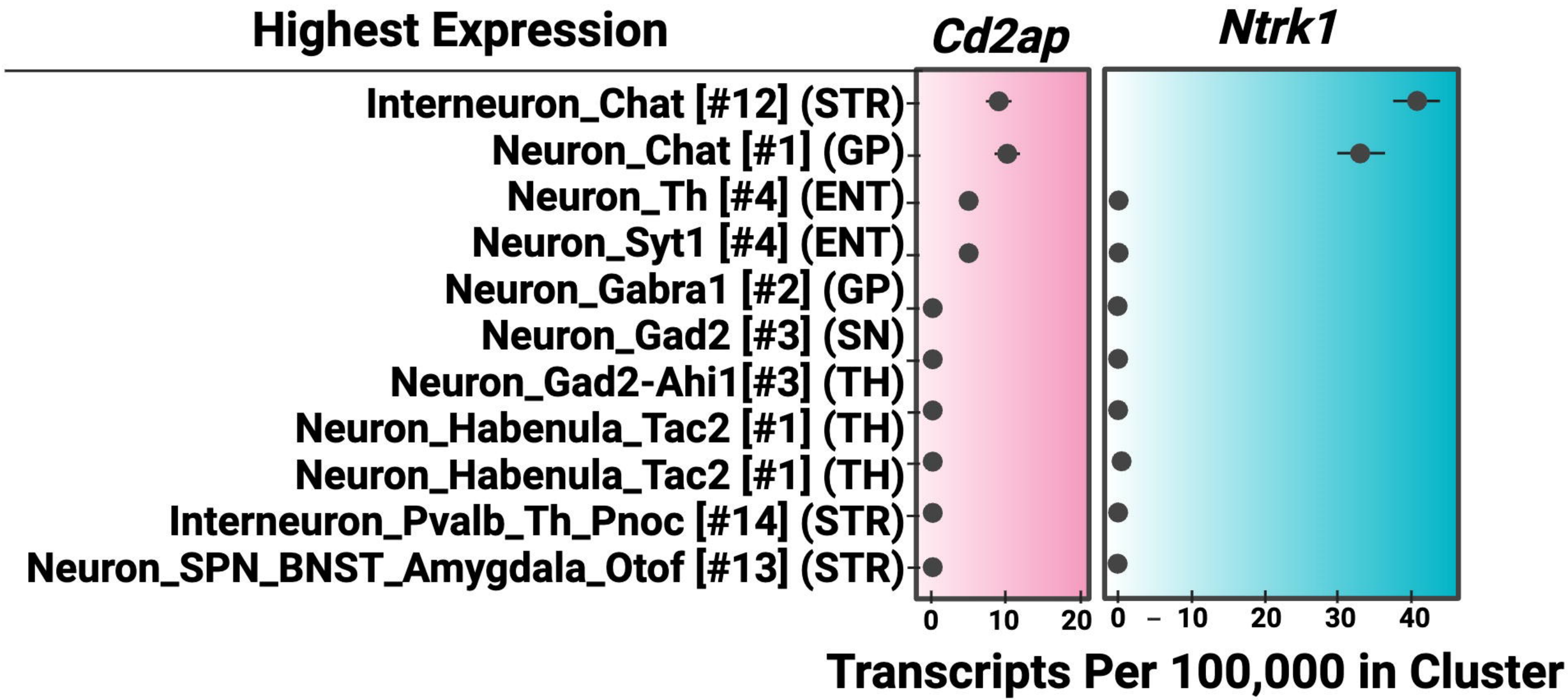
Highest Expression
Cd2ap
Ntrk1
Interneuron_Chat [#12] (STR)
Neuron_Chat [#1] (GP)
Neuron_Th [#4] (ENT)
Neuron_Syt1 [#4] (ENT)
Neuron_Gabra1 [#2] (GP)
Neuron_Gad2 [#3] (SN)
Neuron_Gad2-Ahi1[#3] (TH)
Neuron_Habenula_Tac2 [#1] (TH)
Neuron_Habenula_Tac2 [#1] (TH)
Interneuron_Pvalb_Th_Pnoc [#14] (STR)
Neuron_SPN_BNST_Amygdala_Otof [#13] (STR)
0
10
20
0
10
20
30
40
Transcripts Per 100,000 in Cluster

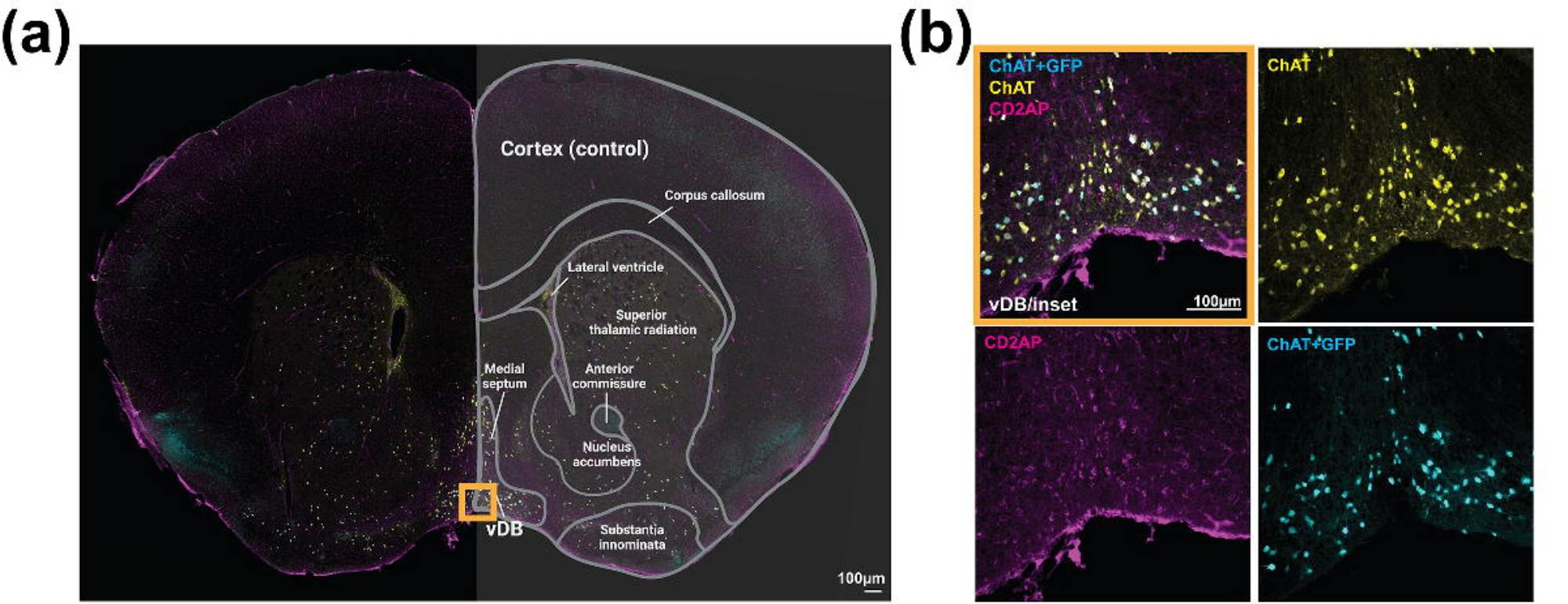
(a)
Cortex (control)
Corpus callosum
Lateral ventricle
Superior thalamic radiation
Medial septum
Anterior commissure
Nucleus accumbens
vDB
Substantia innominata
100µm
(b)
ChAT+GFP
ChAT
CD2AP
vDB/inset
100µm
ChAT
CD2AP
ChAT+GFP

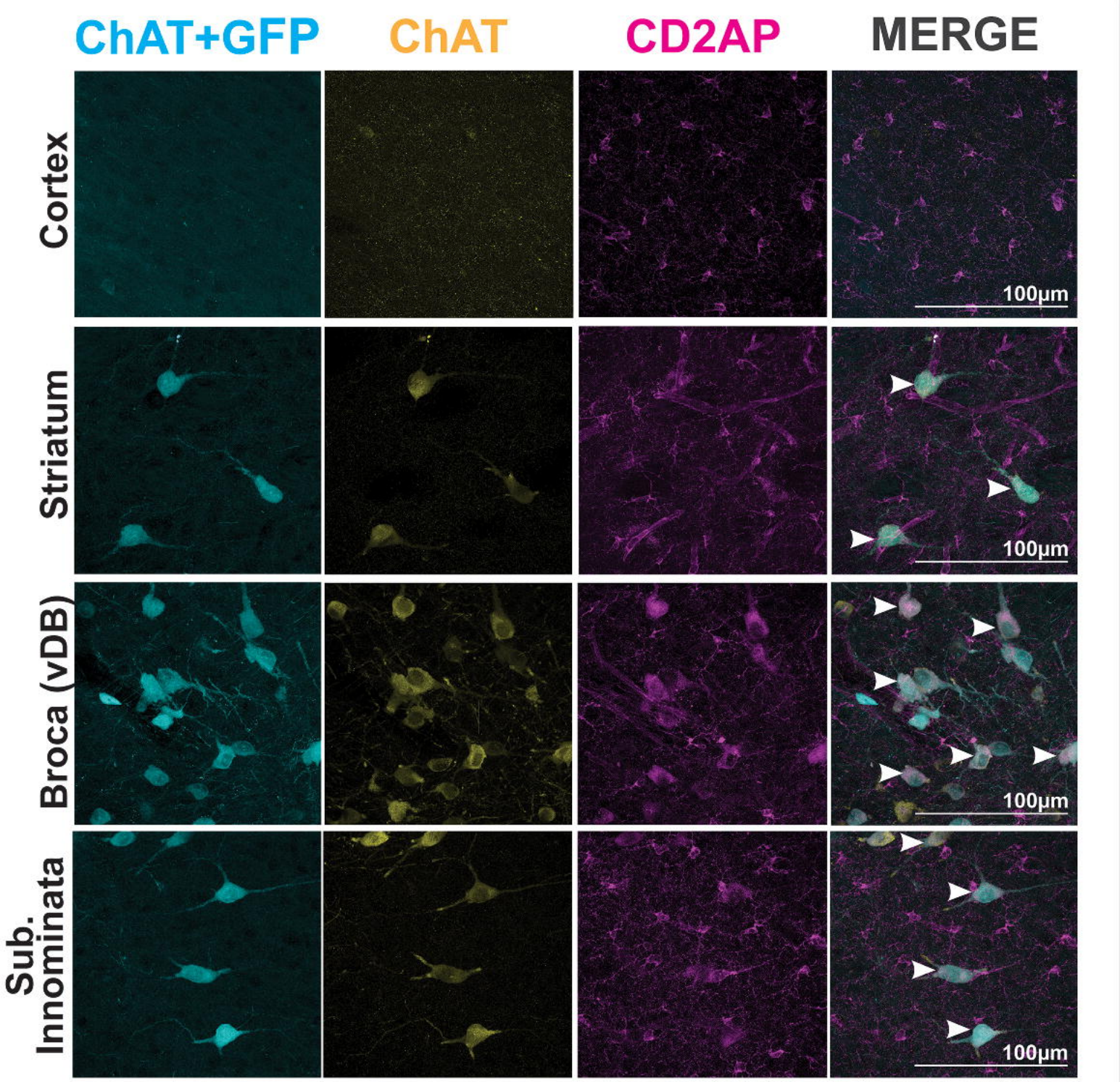
ChAT+GFP
ChAT
CD2AP
MERGE
Cortex
Striatum
Broca (vDB)
Sub. Innominata
100µm
100µm
100µm
100µm

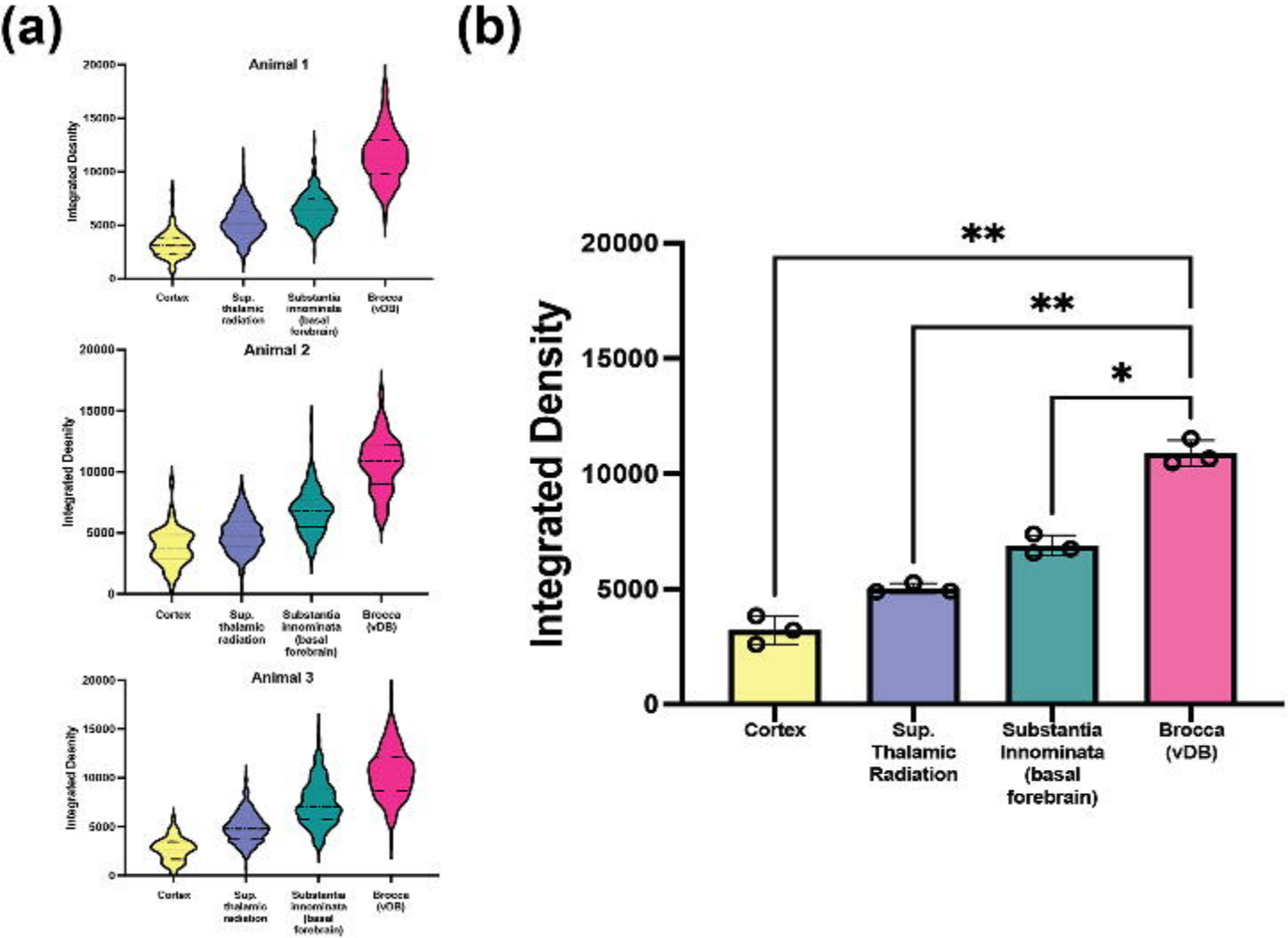
(a)
Animal 1
Animal 2
Animal 3
Integrated Density
20000
15000
10000
5000
0
Cortex
Sup. thalamic radiation
Substantia innominata (basal forebrain)
Brocca (vDB)
(b)
Integrated Density
20000
15000
10000
5000
0
**
**
*
Cortex
Sup. Thalamic Radiation
Substantia Innominata (basal forebrain)
Brocca (vDB)

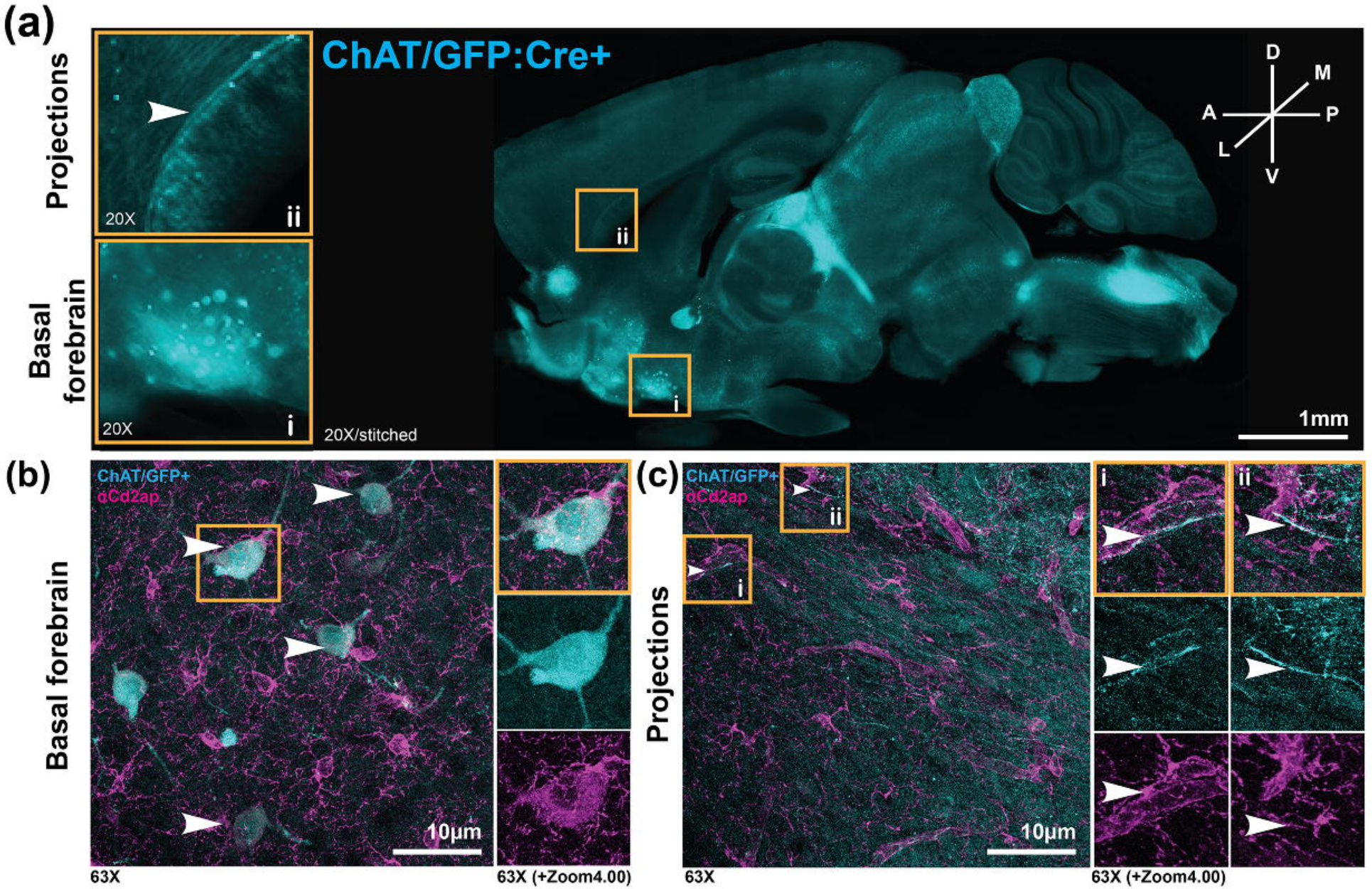
(a)
ChAT/GFP:Cre+
Projections
Basal forebrain
20X
ii
20X
i
20X/stitched
D
M
A
P
L
V
1mm
(b)
ChAT/GFP+
αCd2ap
Basal forebrain
10μm
63X
63X (+Zoom4.00)
(c)
ChAT/GFP+
αCd2ap
Projections
10μm
63X
63X (+Zoom4.00)

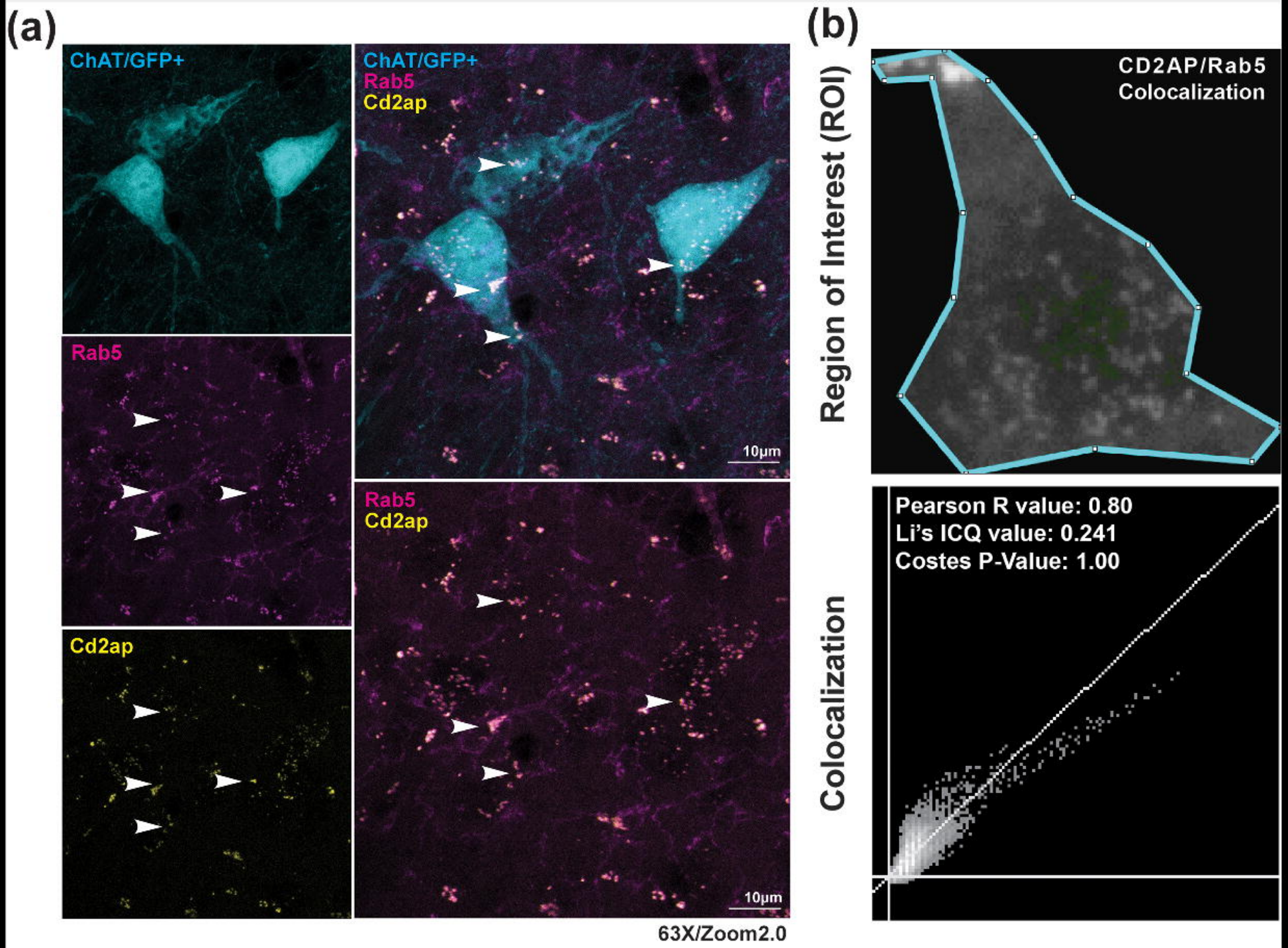
(a)
ChAT/GFP+
Rab5
Cd2ap
ChAT/GFP+
Rab5
Cd2ap
10µm
Rab5
Cd2ap
10µm
63X/Zoom2.0
(b)
Region of Interest (ROI)
CD2AP/Rab5
Colocalization
Colocalization
Pearson R value: 0.80
Li's ICQ value: 0.241
Costes P-Value: 1.00